A Novel Tumor-Promoting Function Residing in the 5′ Non-coding Region of *vascular endothelial growth factor* mRNA

Kiyoshi Masuda, Shigetada Teshima-Kondo*, Mina Mukaijo, Naoko Yamagishi, Yoshiko Nishikawa, Kensei Nishida, Tomoko Kawai, Kazuhito Rokutan

Department of Stress Science, Institute of Health Biosciences, University of Tokushima Graduate School, Tokushima, Japan

Funding: This work was supported in part by grants from Grants-in-Aid for Scientific Research C (16590598) and Grants-in-Aid for Exploratory (19659187) from Japan Society for the Promotion of Science (JSPS) and Grants-in-Aid for Young Scientists A (18689018) from the Ministry of Education, Culture, Sports, Science, and Technology of Japan (to ST-K), and from Grants-in-Aid for Scientific Research B (17390218) from the JSPS (to KR). The funders had no role in study design, data collection and analysis, decision to publish, or preparation of the manuscript.

Competing Interests: The authors have declared that no competing interests exist.

Academic Editor: Pam Jones, University of Leeds, United Kingdom

Citation: Masuda K, Teshima-Kondo S, Mukaijo M, Yamagishi N, Nishikawa Y, et al. (2008) A novel tumor-promoting function residing in the 5′ non-coding region of *vascular endothelial growth factor* mRNA. PLoS Med 5(5): e94. doi:10.1371/journal.pmed.0050094

Received: October 5, 2007
Accepted: March 13, 2008
Published: May 20, 2008

Abbreviations: CAT, chloramphenicol acetyltransferase; CHX, cycloheximide; 5-FU, 5-fluorouracil; GAS, IFN-γ-activated sequence; IFN, interferon; ISRE, IFN-stimulated regulatory element; nt, nucleotide; PKR, RNA-activated protein kinase; rh, recombinant human; RT-PCR, real-time PCR; SEM, standard error of the mean; siRNA, small-interfering RNA; STAT, signal transducers and activators of transcription; UTR, untranslated region; VEGF, vascular endothelial growth factor-A; VEGFR, vascular endothelial growth factor receptor; YFP, yellow fluorescent protein; Ab, antibody

* To whom correspondence should be addressed. E-mail: kondoshi@basic.med.tokushima-u.ac.jp

ABSTRACT

Background

Vascular endothelial growth factor-A (VEGF) is one of the key regulators of tumor development, hence it is considered to be an important therapeutic target for cancer treatment. However, clinical trials have suggested that anti-VEGF monotherapy was less effective than standard chemotherapy. On the basis of the evidence, we hypothesized that *vegf* mRNA may have unrecognized function(s) in cancer cells.

Methods and Findings

Knockdown of VEGF with *vegf*-targeting small-interfering (si) RNAs increased susceptibility of human colon cancer cell line (HCT116) to apoptosis caused with 5-fluorouracil, etoposide, or doxorubicin. Recombinant human $VEGF_{165}$ did not completely inhibit this apoptosis. Conversely, overexpression of $VEGF_{165}$ increased resistance to anti-cancer drug-induced apoptosis, while an anti-$VEGF_{165}$-neutralizing antibody did not completely block the resistance. We prepared plasmids encoding full-length *vegf* mRNA with mutation of signal sequence, *vegf* mRNAs lacking untranslated regions (UTRs), or mutated 5′UTRs. Using these plasmids, we revealed that the 5′UTR of *vegf* mRNA possessed anti-apoptotic activity. The 5′UTR-mediated activity was not affected by a protein synthesis inhibitor, cycloheximide. We established HCT116 clones stably expressing either the *vegf* 5′UTR or the mutated 5′UTR. The clones expressing the 5′UTR, but not the mutated one, showed increased anchorage-independent growth in vitro and formed progressive tumors when implanted in athymic nude mice. Microarray and quantitative real-time PCR analyses indicated that the *vegf* 5′UTR-expressing tumors had up-regulated anti-apoptotic genes, multidrug-resistant genes, and growth-promoting genes, while pro-apoptotic genes were down-regulated. Notably, expression of signal transducers and activators of transcription 1 (STAT1) was markedly repressed in the 5′UTR-expressing tumors, resulting in down-regulation of a STAT1-responsive cluster of genes (43 genes). As a result, the tumors did not respond to interferon (IFN)α therapy at all. We showed that stable silencing of endogenous *vegf* mRNA in HCT116 cells enhanced both STAT1 expression and IFNα responses.

Conclusions

These findings suggest that cancer cells have a survival system that is regulated by *vegf* mRNA and imply that both *vegf* mRNA and its protein may synergistically promote the malignancy of tumor cells. Therefore, combination of anti-*vegf* transcript strategies, such as siRNA-based gene silencing, with anti-VEGF antibody treatment may improve anti-cancer therapies that target VEGF.

The Editors' Summary of this article follows the references.

Introduction

Vascular endothelial growth factor-A (VEGF) is one of the key regulators in tumor formation and progression [1–4]. The clinical significance of VEGF in tumors has been demonstrated by many studies showing that the VEGF expression level is correlated with tumor grade, depth of invasion, status of nodal and distant metastasis, and clinical stage [5–10]. In addition, high levels of circulating VEGF are associated with resistance to chemotherapy in patients with metastatic solid tumors, including colorectal cancer [11,12]. The stimulatory action of VEGF on tumor angiogenesis is believed to play a central role in promotion of tumor development. At the same time, VEGF is known to act as an autocrine survival and growth factor for tumor cells [13]. Based on the evidence outlined above, a number of strategies to target VEGF or VEGF receptors (VEGFR) have been developed and subjected to clinical evaluation [14]. In contrast to preclinical studies in animal models, clinical trials suggest that anti-VEGF monotherapy was less effective than standard chemotherapy [15], raising the possibility that VEGF or possibly *vegf* mRNA might possess unrecognized function(s).

A recent report has shown that VEGF protein functions as an internal autocrine survival factor in human breast cancer cells through internally expressed VEGFR [16]. In addition, non-coding RNAs have now been recognized to play critical roles in tumorigenesis [17]. One class of the tumor-associated non-coding RNAs is the untranslated region (UTR) of certain mRNAs, including the 3′UTR of α-*tropomyosin* mRNA [18], the 3′UTR of *prohibitin* mRNA [19], the 3′UTR of *ribonucleotide reductase* mRNA [20], and the 5′UTR of *c-myc* mRNA [21]. All of these UTR RNAs function as tumor suppressors. From this point of view, we directed our attention to a unique structure of *vegf* mRNA characterized by its unusually long 5′UTR (1,038 nucleotide [nt]) containing two internal ribosome entry sites (IRES) [22,23].

Methods

Reagents

Recombinant human (rh) interferon alpha (IFNα) was purchased from PBL Biomedical Laboratories. rhIFNγ, rhVEGF$_{165}$, and anti-VEGF$_{165}$-neutralizing monoclonal antibody (Ab) were from R&D Systems.

Cell Culture and Transfection

The human colon carcinoma cell lines (HCT116 and RKO) were maintained in McCoy's 5A medium, supplemented with 10% (v/v) FCS and antibiotics. The human embryonic kidney cell line (HEK293) was maintained in DMEM medium, supplemented with 10% (v/v) FCS and antibiotics. The human gastric carcinoma cell line (AGS) was maintained in F-12 medium, supplemented with 10% (v/v) FCS and antibiotics. Amounts of VEGF$_{165}$ secreted into the culture medium were measured by ELISA assay (Quantikine, R&D Systems), according to the manufacturer's instructions.

Transfection of cells was performed using the jetPEI (Polyplus-transfection) or FuGENE HD (Roche Diagnostics) transfection reagent, according to the manufacturer's instructions. We checked the transfection efficiency by monitoring expression of yellow fluorescent protein (YFP)-expressing plasmid and determined the efficiency to be 60%–65% in HCT116 cells, 80%–85% in HEK293 cells, 60%–65% in RKO cells, and 60%–65% in AGS cells.

Cell Growth

Cell growth was assessed using a CellTiter 96 AQueous One Solution Cell Proliferation Assay (Promega), according to the manufacturer's instructions. Cells were plated in a 96-well flat-bottom plate and cultured in 100 μl of McCoy's 5A medium containing 10% (v/v) FCS and antibiotics, and the MTT reagent (20 μl/well) was added to each well and incubated for 1 h. The levels of blue formazan were measured spectrophotometrically at 490 nm at each time point using a microplate reader (Wallac 1420 ARVO MX; Perkin Elmer).

To assess anchorage-independent growth, cells (1×10^5) were plated in 2 ml of McCoy's 5A medium containing 10% (v/v) FCS and 0.33% agar. This suspension was layered over a 3-ml base layer of solidified McCoy's medium containing 10% (v/v) FCS and 0.5% agar in 60-mm diameter culture dishes. Following a 28-d incubation at 37 °C in 5% CO_2, the number of colonies (approximately >0.1 mm in diameter) with dense centers was scored for each plate.

Assessment of Apoptosis

Apoptotic cells were assessed by the TUNEL-staining method using an in situ Cell Death Detection kit (Roche Diagnostics). TUNEL-positive cells were viewed using a microscope, and percentages of the positive cells were calculated. A minimum of 300 cells was counted for each determination. Apoptosis was also detected using the APOPercentage apoptosis assay kit (Biocolor), according to the manufacturer's instructions. The APOPercentage dye stains cells undergoing the membrane "flip-flop" event when phosphatidylserine is translocated to the outer leaflet. This event is specific for apoptosis, but not for necrosis.

The caspase 3/7 activity was measured using the Caspase-Glo 3/7 assay (Promega), according to the manufacturer's instructions. After cells were treated with 80 μM of 5-fluorouracil (5-FU) for 24 h, the Caspase-Glo 3/7 reagent was added to each well and incubated for 1 h. The luminescence was measured using a microplate-reading luminometer (Wallac 1420 ARVO MX; Perkin Elmer).

Plasmid Constructions and Establishment of Stable Transfectants

The plasmids expressing *vegf* small-interfering RNAs (siRNAs) were constructed using a BLOCK-iT Pol II miR RNAi expression vector kit (Invitrogen), in accordance with the manufacturer's protocol. A pcDNA6.2-GW/EmGFP-miRNA vector that contains the GFP-coding region within the pre-miRNA expression cassette was inserted with the following pairs of sense and antisense DNA: *vegf* siRNA number 1, 5′-TGC TGA GCA AGG CAA GGC TCC AAT GCG TTT TGG CCA CTG ACT GAC GCA TTG GAC TTG CCT TGC T-3′ (sense) and 5′-AGC AAG GCA AGT CCA ATG CGT CAG TCA GTG GCC AAA ACG CAT TGG AGC CTT GCC TTG CTC AGC A-3′ (antisense); *vegf* siRNA number 2, 5′-TGC TGA GAG CAG CAA GGC AAG GCT CCG TTT TGG CCA CTG ACT GAC GGA GCC TTC TTG CTG CTC T-3′ (sense) and 5′-AGA GCA GCA AGA AGG CTC CGT CAG TCA GTG GCC AAA ACG GAG CCT TGC CTT GCT GCT CTC AGC A-3′ (antisense). These siRNAs were cloned into pcDNA6.2-GW/EmGFP-miRNA vector (siVEGF#1 and siVEGF#2 in Figure 1).

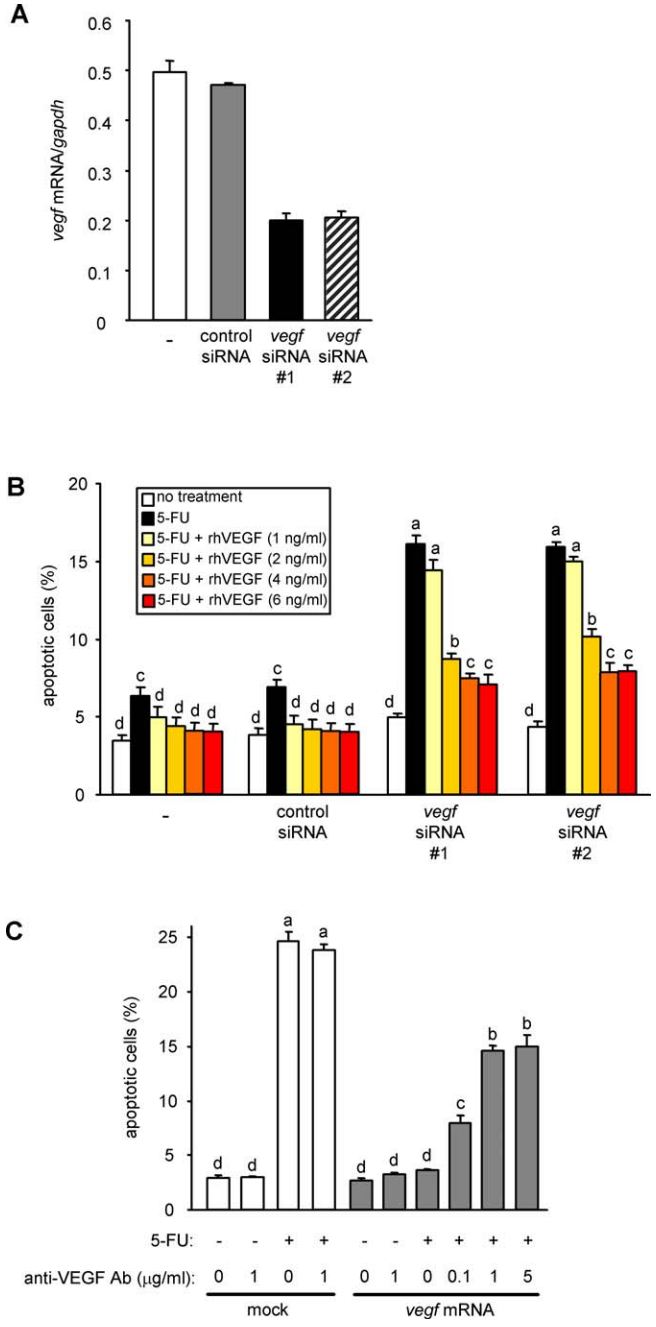

Figure 1. Effect of *vegf* Transcript on Susceptibility to Anti-Cancer Drugs

(A) Knockdown efficiency of *vegf* mRNA. Expression levels of *vegf* mRNA were measured using quantitative RT-PCR. Values were normalized for the amount of *gapdh* mRNA (means ± SEM, $n = 4$).

(B) Knockdown of *vegf* mRNA increases 5-FU induced apoptosis. Cells untransfected (–) or transfected with the indicated plasmids for 24 h were treated with 20 μM 5-FU or rhVEGF protein (1, 2, 4, or 6 ng/ml) combined with 5-FU (20 μM) for 48 h. Apoptosis was evaluated by calculating the percentages of TUNEL-positive cells. Values are means ± SEM from four independent experiments. Means with different superscripts are significantly different by ANOVA followed by Scheffé's test ($p < 0.05$).

(C) Overexpression of *vegf* transcript induces resistance to 5-FU. Cells were transfected with a plasmid encoding full-length *vegf* mRNA or an empty vector (mock) for 24 h. The cells were treated without or with 80 μM 5-FU in the presence of a monoclonal anti-human $VEGF_{165}$-neutralizing Ab at the indicated concentrations for 48 h, and then apoptotic cells were identified and quantitated by the TUNEL-staining method. Values are means ± SEM from three independent experiments. Means with different superscripts are significantly different by ANOVA followed by Scheffé's test ($p < 0.05$).

doi:10.1371/journal.pmed.0050094.g001

As a control siRNA-expressing plasmid, we used the pcDNA6.2-GW/EmGFP-miR-negative control plasmid expressing mature siRNA that is predicted not to target any known vertebrate genes (Invitrogen).

The following plasmid constructs were kindly provided by Drs. Hervé Prats and Anne-Catherine Prats [24–27]: pAUG165mSPHA (construct I in Figure 2A), p165mSPHA 3′ (construct II), pVC (construct V), pSCT-chloramphenicol acetyltransferase (CAT) (construct IX), pVCTTT (construct XI), the plasmids expressing a chimeric mRNA fused to CAT coding sequence comprising one of the constructs (the human *bip* 5′UTR, the human *c-myc* 5′UTR, the human *fgf-2* 5′UTR, and the human *pdgf-b* 5′UTR), and the bicistronic plasmid contains two luciferase genes, *Renilla* luciferase (LucR) and firefly luciferase (LucF), which are separated by a hairpin (hairpin control) or an IRES of human *bip* (pRBL), human *c-myc* (pRMyP2L), and human *fgf-2* (pRFL).

p165mSPHA 3′ and p165AUGmSPHA have H9D and L14E mutations in the signal sequence that prevent secretion of the $VEGF_{165}$ protein. p165mSPHA 3′ was digested with ClaI and ApaI, blunted by Klenow treatment, and religated. The resulting plasmid (p165mSPHA, construct III in Figure 2A) did not contain the 3′UTR sequence. p165mSPHA 3′ was digested with XbaI and NgoMIV, blunted by Klenow treatment, and religated. The resulting plasmid (pAUG165mSPHA 3′, construct IV) did not encode the 5′UTR sequence. Several deletion constructs of the *vegf* 5′UTR were also made from the pVC plasmid by digestion with NgOMIV (construct VI), XbaI and NheI (construct VII), or BamHI (construct VIII). We also prepared a plasmid encoding full-length *vegf* mRNA with an intact signal peptide sequence. The construct pVC, which has an intact signal sequence, was digested with NarI and BsaBI, and the resultant NarI-BsaBI fragment was ligated into p165mSPHA 3′ to reconstruct full-length *vegf* mRNA with an intact signal peptide sequence (p165HA 3′). A construct mutated between nt 591 and nt 746 of the *vegf* 5′UTR was synthesized using two serial double-stranded DNA fragments (mutations are indicated by lower case letters): nt 576 -GCG AGC CGC GGG CAa GGa CCa GAa CCa GCa CCa GGg GGa GGa GTa GAa GGa GTa GGG GCT C- nt 636 and nt 637- GGGCT CGa GGa GTa GCa tta AAg CTa TTt GTa CAg tta tta GGa TGc TCa CGa TTt GGg GGg GCa GTa GTa aga GCa GGa GAg GCa GAa CCa AGt GGg GCa GCa AGg AGT GCT AGC- nt 752. The two synthesized fragments were ligated and inserted into pVC digested with SacII and NheI to generate plasmid pVCmut (construct X in Figure 2A). All the constructs were confirmed to have the expected sequences using a DNA sequencer. The secondary structures of *vegf* 5′UTR and its mutant were analyzed using the mfold 3.2 algorithm of Zuker [28].

We also constructed a plasmid expressing a chimeric mRNA comprising the *vegf* 5′UTR fused to YFP. The constructs pVC and pVCmut were digested with EcoRI and NcoI, and the resulting EcoRI-NcoI fragments were ligated into pd2EYFP-N1 (Clontech) to generate pVY and pVYmut, respectively.

Stable transfectants were constructed using early passages of HCT116 cells that had been plated at approximately 1×10^5 in a 60-mm diameter culture dish and cultured overnight. The cells were transfected with 5 μg of pYFP, pVY, pVYmut, siVEGF#1, or pcDNA6.2-GW/EmGFP-miRNA-neg control plasmids. Clones were selected and maintained in McCoy's 5A medium supplemented with 450 μg/ml G418 (Invitrogen), or with 5 μg/ml Blasticidin (Invitrogen). Three stably transfected cell lines (HCT116/YFP, HCT116/*vegf* 5′, HCT116/*vegf*

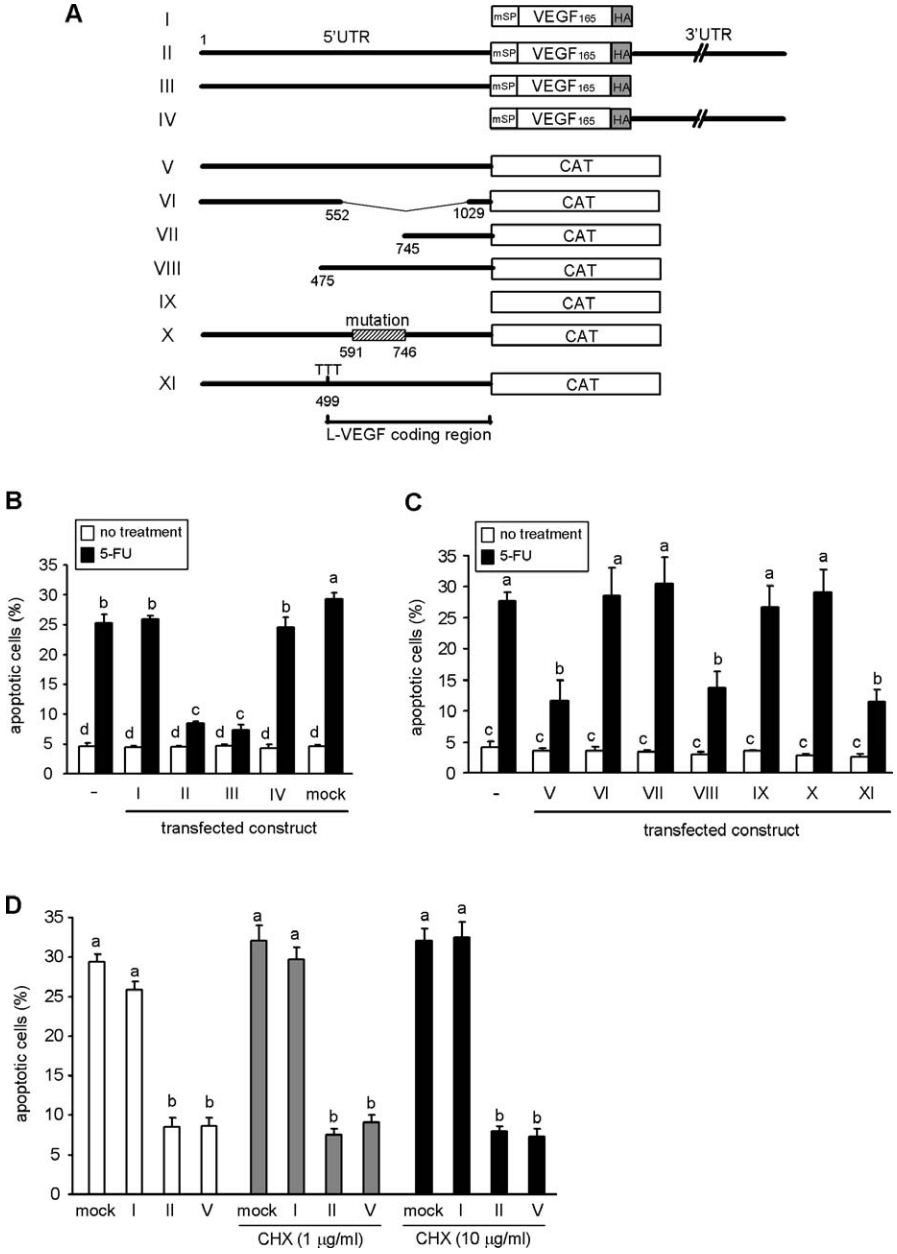

Figure 2. Effects of *vegf* 5′UTR RNA on Resistance to 5-FU

(A) Schematic of the constructs transfected into HCT116 cells. mSP, mutated signal peptide; HA, hemagglutinin.

(B) The *vegf* 5′UTR induces 5-FU resistance. Cells untransfected (–) or transfected with the indicated construct for 24 h were treated with 80 μM 5-FU for 48 h, and then apoptotic cells were identified and quantitated by the TUNEL-staining method. Values are means ± SEM from three independent experiments. Means with different superscripts are significantly different by ANOVA followed by Scheffé's test ($p < 0.05$).

(C) Determination of functional element in the *vegf* 5′UTR. Cells untransfected (–) or transfected with the indicated construct for 24 h were treated with 80 μM 5-FU for 48 h. Apoptotic cells was then measured by the TUNEL-staining method as described above. Values are means ± SEM from three independent experiments. Means with different superscripts are significantly different by ANOVA followed by Scheffé's test ($p < 0.05$).

(D) The *vegf* 5′UTR-mediated resistance to 5-FU is independent of de novo protein synthesis. Cells transfected with the indicated plasmids for 24 h were treated with 80 μM 5-FU in the absence or presence of CHX (1 or 10 μg/ml) for 40 h. Apoptosis was assessed by the TUNEL-staining method. Values are means ± SEM from four independent experiments. Means with different superscripts are significantly different by ANOVA followed by Scheffé's test ($p < 0.05$).

doi:10.1371/journal.pmed.0050094.g002

5′mut, HCT116/siVEGF, or HCT116/siControl) were isolated after 28 d of selection.

Western and Northern Blot Analyses

Cell lysates were prepared using a lysis buffer containing 100 mM Tris-HCl (pH 6.8), 300 mM NaCl, 2 mM EDTA, and 4% (v/v) SDS. Western immunoblotting was performed as described previously [29] using a rabbit polyclonal anti-human influenza virus hemagglutinin (HA) Ab (Santa Cruz Biotechnology) at a 1/1,000 dilution, a mouse monoclonal Ab against human signal transducers and activators of transcription 1 (STAT1) (Cell Signaling) at a 1/1,000 dilution, a

rabbit polyclonal anti-L-VEGF Ab at a 1/500 dilution (a gift from Hervé Prats) [26], or a mouse anti-β-actin monoclonal Ab (Sigma). The specificity of individual antibody reactivity was confirmed by the absorption test with the corresponding antigen peptide (Figure S10). Blocking antigen peptide for human STAT1 and HA were obtained from Cell Signaling and Santa Cruz Biotechnology, respectively. Antigen peptides for L-VEGF were synthesized using an Applied Biosystems 432A peptide synthesizer.

Total RNA was prepared by the guanidinium thiocyanate method. Northern hybridization was performed as described previously [29] using following cDNA probes. cDNA probes for *vegf* 5′UTR RNA and *vegf* ORF RNA were prepared by digestion of the plasmid p165mSPHA 3′ with NgoMIV and ClaI, and SacII and NheI, respectively. A cDNA probe for CAT mRNA was prepared as a digestion fragment of the plasmid pVC using EcoRI and BglII sites. These probes were labeled with [α-^{32}P]dCTP using Klenow enzyme (New England BioLabs), according to the manufacturer's instructions.

Animal Studies and Immunohistochemistry

The use of animals in the experiments described here was approved by the Animal Care Committee of University of Tokushima. Seven-wk-old male athymic nude mice (Nippon SLC) were caged in groups of five and acclimated for 1 wk. A cell suspension (5×10^6 cells) in serum-free McCoy's 5A medium, prepared from each stably transfected clone, was injected subcutaneously into the flanks of nude mice. The sizes of tumors that developed in the injected mice were measured in two dimensions with a caliper and their volumes calculated using the formula $(L \times W^2) \times 0.5$, where L is length and W is width. We confirmed that parental HCT116 cells (5×10^6 cells) injected subcutaneously into nude mice formed tumors whose volumes were around 500 mm^3 day 28 after transplantation. Therefore, HCT116/YFP clones appeared to form xenograft tumors less efficiently than parental HCT116 cells, probably because expression of YFP and/or procedures during the establishment of permanent cell cloning was likely to nonspecifically reduce the tumor-forming capability.

Some mice were injected intraperitoneally with BrdU (1.5 g/kg body weight, Sigma-Aldrich) 2 h before they were humanely killed. The mice were killed on the indicated days, and growing tumors were removed and fixed with formalin in PBS. The fixed xenografts were sectioned and stained with hematoxylin and eosin (HE), or by immunohistochemistry using a mouse monoclonal anti-BrdU Ab (Sigma-Aldrich), or by a DeadEnd colorimetric TUNEL System (Promega). Vasculature was stained using a rat anti-mouse CD31 Ab (BD Pharmingen).

We also examined the effects of 5-FU on implanted tumors. In this experiment, HCT116/*vegf* 5′ transfectants (5×10^6 cells) were injected subcutaneously into the left flanks of nude mice, and HCT116/YFP (1×10^7 cells) or HCT116/*vegf* 5′mut transfectants (1×10^7 cells) were injected into the right flanks of the same mice. When the tumors reached a size of approximately 40 mm^3, usually by day 7, the mice were treated daily with an intraperitoneal injection of 5-FU (30 mg/kg weight, Sigma-Aldrich), or with 5-FU (30 mg/kg weight) plus IFNα (50,000 U/mouse; PBL Biomedical Laboratories). The tumor sizes were measured daily using a caliper, and their volumes were calculated as described above.

Microarray Analysis

We used Agilent Human 1A oligomicroarrays (Agilent Technologies) containing 60-mer DNA probes synthesized in situ in a 22-k format. Total RNA was prepared from three independent *vegf* 5′-G5 tumors on day 14, and an equal amount of RNA from each tumor was mixed. After contaminating DNA had been removed using a DNase kit (Qiagen), the resultant RNA quality was evaluated using the Agilent 2100 Bioanalyzer (Agilent Technologies). Total RNA was also prepared from three *vegf* 5′mut-D5 tumors on day 14 in the same manner. Synthesis, amplification, and labeling of cRNA were carried out in accordance with the manufacturer's protocol. Cy5-cRNA (0.75 μg) prepared from *vegf* 5′-G5 tumors was mixed with the same amount of Cy3-cRNA from *vegf* 5′mut-D5 tumors. Hybridization was performed on the Agilent Human 1A oligomicroarray (Agilent Technologies), according to the manufacturer's protocol. Fluorescence images of the hybridized microarrays were obtained using an Agilent microarray scanner (G2565BA). Signal intensities of Cy5 and Cy3 were quantified and analyzed by subtracting the backgrounds using feature extraction software (Agilent, version 9.5). The Cy5/Cy3 ratios of 12,178 genes that had a higher fluorescence value than 100 for both Cy5 and Cy3 signals were transformed to logarithms for global normalization. We selected genes whose mRNA levels differed by >2-fold between *vegf* 5′-G5 and mut-D5 tumors.

Dual-Luciferase Assay

To measure IRES activity, we used the bicistronic plasmid. The bicistronic cassette expresses the LucR in a cap-dependent manner and LucF in an IRES-dependent manner. Each IRES or hairpin control is located between the two cistrons.

To measure IFN-dependent transcriptional activity, we used plasmids containing the motifs IFN-stimulated regulatory element (ISRE) and IFN-γ-activated sequence (GAS) upstream of the LucF reporter gene (Pathway Profiling Luciferase System).

LucF and LucR activities were measured using the Dual-Luciferase reporter assay system (Promega), according to the manufacturer's instructions. Transfected cells were rinsed twice with PBS, scraped, and homogenized in 50 μl of lysis reagent provided with the kit. The lysate was cleared by a 2-min centrifugation at 4 °C. Chemiluminescent signals were measured in a luminometer (Wallac 1420 ARVO MX; Perkin Elmer) equipped with automatic injectors.

Quantitative Real-Time PCR

SuperScript II RNase H-reverse transcriptase (Invitrogen) was used to synthesize cDNAs from 1 μg aliquots of total RNA prepared from three independent tumor tissues. Taqman Gene Expression assays (Applied Biosystems) were used with the following cDNA-specific primers and probes: *mia* (Hs00197954__m1); *bcl6* (Hs00153368__m1); *egfr* (Hs00193306__m1); *nrg1* (Hs00247624__m1); *pcdc1* (Hs00169472__m1); *fas* (Hs00531110__m1); *bax* (Hs00180269__m1); *xaf1* (Hs00213882__m1); *trail/apo2* (Hs00234356__m1); *nmi* (Hs00190768__m1); *isg20* (Hs00158122__m1); *oas1* (Hs00242943__m1); *oas2* (Hs00213443__m1); *irf1* (Hs00233698__m1); *pml* (Hs00231241__m1); and *gapdh* (Hs99999905__m1). The levels of transcripts for IFN receptors (*ifnar1*, *ifnar2*, *ifngr1*, and *ifngr2*), VEGF receptors (*vegfr1*, *vegfr2*, *nrp1* and *nrp2*), *stat1*,

vegf, and β-actin were measured by real time (RT)-PCR using the following specific primer sets: *ifnar1*, 5′-CCC AGT GTG TCT TTC CTC AAA-3′ (forward) and 5′-AAG ACT GGA GGA AGT AGG AAA GC-3′ (reverse); *ifnar2*, 5′-AGT CAG AGG GAA TTG TTA AGA AGC A-3′ (forward) and 5′-TTT GGA ATT AAC TTG TCA ATG ATA TAG GTG-3′ (reverse); *ifngr1*, 5′-GGT GTG AGC AGG GCT GAG-3′ (forward) and 5′-GTA ACA TTA GTT GGT GTA GGC ACT G-3′ (reverse); *ifngr2*, 5′-GGC CTG ATT AAA TAC TGG TTT CA-3′ (forward) and 5′-GGG CTG AGT TGG GTC TTT TA-3′ (reverse); *vegfr1*, 5′-AGA ACC CCG ATT ATG TGA GAA A-3′ (forward) and 5′-GAT AGA TTC GGG AGC CAT CC-3′ (reverse); *vegfr2*, 5′-GAA CAT TTG GGA AAT CTC TTG C-3′ (forward) and 5′-CGG AAG AAC AAT GTA GTC TTT GC-3′ (reverse); *nrp1*, 5′-CCC TGA GAA TGG GTG GAC T-3′ (forward) and 5′-CGT GAC AAA GCG CAG AAG-3′ (reverse); *nrp2*, 5′-GGA CCC CCA ACT TGG ATT-3′ (forward) and 5′-ATG GTT AAA AAG CGC AGG TC-3′ (reverse); *stat1*, 5′-CTG CTC CTT TGG TTG AAT CC-3′ (forward) and 5′-GCT GAA GTT CGT ACC ACT GAG A-3′ (reverse); *vegf*, 5′-GAG CCT TGC CTT GCT GCT CTA C-3′ (forward) and 5′-CAC CAG GGT CTC GAT TGG ATG-3′ (reverse); β-actin, 5′-CCA ACC GCG AGA AGA TGA-3′ (forward) and 5′-CCA GAG GCG TAC AGG GAT AG-3′ (reverse). Amplification and quantification of the PCR products were performed using the Applied Biosystems 7500 System (Applied Biosystems). Standards were run in the same plate and the relative standard curve method was used to calculate the relative mRNA expression. RNA amounts were normalized against the *gapdh* mRNA level.

Statistical Analysis

The data were analyzed using the two-tailed Student's *t*-test or ANOVA and the Scheffé's test. A *p*-value of less than 0.05 was considered significant.

Results

Effect of *vegf* mRNA on Apoptosis Caused with Anti-Cancer Drugs

First, we investigated whether *vegf* mRNA possessed a tumor-promoting activity in HCT116 cells that expressed VEGFR-2 and Neuropilin-1, −2 (Figure S6) and secreted spontaneously $VEGF_{165}$ at 759 ± 32 pg/ml (mean ± SD, $n = 4$). Two different *vegf*-targeting siRNAs successfully knocked down endogenous *vegf* mRNA in HCT116 cells (Figure 1A). This silencing made the cells susceptible to apoptosis caused with a low concentration of 5-FU (20 μM). We then examined the effect of supplementation of $rhVEGF_{165}$ in the knockdown cells. The amount of secreted $VEGF_{165}$ increased to 1,018 ± 48 ($n = 4$) from the cells that were untransfected and treated with 5-FU (20 μM) for 48 h. An external supplementation of 1,000 pg/ml $rhVEGF_{165}$ failed to block the 5-FU-induced apoptosis in *vegf* siRNA-transfected cells (Figure 1B). Treatment with $rhVEGF_{165}$ at 2,000 pg/ml or higher significantly, but not completely, prevented the apoptosis.

In contrast, cells were transiently transfected with a plasmid expressing full-length $vegf_{165}$ mRNA and exposed to a higher concentration of 5-FU (80 μM). These cells secreted $VEGF_{165}$ (7,092 ± 23 pg/ml, $n = 4$) during the experimental period and exhibited resistance to 5-FU-induced apoptosis (Figure 1C). It should be noted that anti-$VEGF_{165}$-neutralizing monoclonal Ab could not completely cancel the anti-apoptotic activity even at concentrations of up to 5 μg/ml (about 250 molar excess amount of secreted $VEGF_{165}$) (Figure 1C). Both knockdown and overexpression experiments suggest that both VEGF protein and *vegf* mRNA may possess an anti-apoptotic function. Similar or even clearer results were observed in the cells treated with other anti-cancer drugs, etoposide and doxorubicin (Figure S1A and S1B).

Effect of *vegf* mRNA 5′UTR on Apoptosis Caused by 5-FU

Next, we used the mutated full-length $vegf_{165}$ mRNA-expressing plasmid that has mutations of two amino acid residues within the signal peptide, shown as "mSP" in construct II (Figure 2A). This plasmid-derived mRNA is translated into a nonsecreted $VEGF_{165}$ protein [26]. We confirmed that cells transfected with this construct expressed full-length *vegf* mRNA and $VEGF_{165}$ protein (Figure S2A), but did not secrete detectable amounts of the plasmid-derived $VEGF_{165}$ (unpublished data). As was described above, HCT116 cells overexpressing full-length $vegf_{165}$ mRNA without mutation were completely resistant to 80 μM 5-FU (Figure 1C). In contrast, cells transfected with construct II significantly, but not completely, blocked the 5-FU-induced apoptosis (Figure 2B and Figure S3A). This partial loss of anti-apoptotic activity was probably due to the lack of $VEGF_{165}$-secreting activity. Next, we prepared the constructs lacking the 3′UTR (construct III), 5′UTR (construct IV), or both (construct I), and found that the 5′UTR was associated with the chemoresistant phenotype (Figure 2B). Similar results were observed in the cells treated with other anti-cancer drugs, etoposide and doxorubicin (Figure S1C and S1D).

To confirm the functional role of the 5′UTR, we used a plasmid expressing the *vegf* 5′UTR fused to CAT coding gene (Figure 2A, construct V), which does not express VEGF protein. This chimeric mRNA retained the resistance to 5-FU (Figure 2C). We then designed several deletion constructs of the chimeric mRNA (constructs VI–VIII in Figure 2A), and found that the 270-nt-long element delimited by positions nt 475 and nt 745 in the 5′UTR sequence was crucial for the drug-resistance phenotype (Figure 2C). This sequence is just upstream of IRES-A, but does not require the IRES activity [22].

It is known that the 5′UTR of human *vegf* mRNA encodes long N-terminal VEGF proteins (termed L-VEGF) that are translated from CUG codons upstream of and in-frame with the classical AUG start codon [24]. To eliminate the possibility that the L-VEGF proteins might induce the chemoresistance, we designed a mutated 5′UTR construct that produced L-VEGF protein, but modified the RNA structure by substituting the nucleic acid sequence between nt 591 and nt 746 (construct X in Figure 2A). Secondary structures of the *vegf* 5′UTR and its mutated 5′UTR were predicted by mFold program (Figure S5). The mutation changed the secondary structure of several parts and ablated a stem-loop structure that is located in the functional region of the *vegf* 5′UTR (nt 699 to nt 738) as described above. The mutated construct X produced L-VEGF protein (Figure S2B), but did not induce the resistance to 5-FU (Figure 2C). We also used a simply mutated 5′UTR, in which the first CUG codon was substituted into a noninitiating UUU codon (construct XI in Figure 2A) [24]. This mutant did not produce L-VEGF protein (Figure S2B), but was able to induce the resistance as efficiently as did the wild-type 5′UTR (Figure 2C). We further

examined the effect of a protein synthesis inhibitor, cycloheximide (CHX). To determine the inhibitory effect of CHX, HCT116 cells were transfected with plasmid encoding luciferase in the absence or presence of CHX, and luciferase activity was measured. Protein synthesis was blocked by 86 ± 5% (mean ± SD, $n = 3$) and 94 ± 3% (mean ± SD, $n = 3$) with 1 and 10 μg/ml CHX, respectively. As shown in Figure 2D, both full-length *vegf* mRNA (construct II) and *vegf* 5′UTR-CAT mRNA (construct V) efficiently inhibited 5-FU-induced apoptosis even in the presence with 10 μg/ml CHX. These results suggest that the 5′UTR-mediated chemoresistance may not require de novo protein synthesis.

In addition to the TUNEL-staining method, we evaluated the *vegf* 5′UTR-mediated anti-apoptotic effect by the Apopercentage-staining method (Figure S3C) and by measuring activities of caspase 3 and caspase 7 (Figure S3D), which are crucial effector enzymes for apoptosis induced by genotoxic agents. We confirmed that the results obtained by the Apopercentage-staining method were similar to those by the TUNEL assay (Figure S3B and S3C). Cells transfected with construct II, V, and XI significantly, but not completely, blocked the activation of caspase 3/7 (Figure S3D).

To examine whether this anti-apoptotic function is peculiar to *vegf* mRNA 5′UTR, we used three 5′UTRs containing IRES (*c-myc*, *bip*, and *fgf-2* mRNA 5′UTRs) [30] and the *pdgf-b* mRNA 5′UTR that is unusually long, but does not contain IRES activity [31]. After transfection with plasmid expressing one of the indicated 5′UTR-CAT mRNAs, apoptosis was assessed by the TUNEL-staining method. Only the *vegf* 5′UTR induced the resistance to 5-FU among 5′UTRs tested (Figure S4).

We also examined whether the *vegf* 5′UTR similarly induce the chemoresistance in other human cancer cell lines (RKO, HEK293, and AGS cells), and confirmed that both full-length *vegf* mRNA and *vegf* 5′UTR RNA induced 5-FU resistance in these cells. (Figure S6B–S6D). These observations suggest that the *vegf* 5′UTR function is not peculiar to HCT116 cells.

The *vegf* 5′UTR contains IRES sequences that interact with IRES-binding factors and regulate translation initiation in a cap-independent manner [22,23]. Many IRES-containing mRNAs encode proteins that regulate cell growth, differentiation, and apoptosis [30,32]. Thus, overexpression of the *vegf* 5′UTR raises the possibility that increased amounts of the *vegf* 5′UTR may trap IRES-binding factors, thereby nonspecifically modifying IRES-dependent expression of genes. To address this issue, we tested the effect of *vegf* 5′UTR on other IRES activities (Figure S7B). HCT116 cells were cotransfected with plasmids expressing *vegf* 5′UTR-CAT mRNA (construct V or mutated construct X in Figure 2A) and the bicistronic construct containing 5′UTR of the indicated genes. We confirmed that overexpression of the *vegf* 5′UTR RNA did not repress the IRES activity of *bip*, *c-myc*, or *fgf-2* 5′UTR (Figure S7B).

Characterization of HCT116 Cells Stably Expressing *vegf* 5′UTR

To investigate chronic effects of the *vegf* mRNA 5′UTR on malignant transformation of HCT116 cells both in vitro and in vivo, we established stable transfectants that expressed chimeric mRNAs of either the *vegf* 5′UTR or the mutant one (as described above) fused to the YFP coding gene. Use of these chimeric mRNAs had the following advantages: (i) they did not produce VEGF protein, (ii) expression of these elements could be monitored by YFP fluorescence, and (iii) the chimeric mRNAs were translated similarly as *vegf* mRNA in our cell system. Ectopic mRNAs were equally expressed in corresponding cell lines and did not modify the amounts of endogenous *vegf* mRNA and VEGF among the clones (Figure S8A and S8B).

The *vegf* 5′UTR-expressing cells (HCT116/*vegf* 5′, clones G3 and G5) were again resistant to 5-FU-induced apoptosis (Figure 3A). In contrast, the mutant *vegf* 5′UTR-expressing cells (HCT116/*vegf* 5′mut, clones D5 and E4) or the transfection control cells (HCT116/YFP, clone G11) underwent apoptosis by 5-FU (Figure 3A). We also examined the growth rate of each clone and observed that the HCT116/*vegf* 5′ exhibited a small, albeit significant increase in growth rate compared to the HCT116/*vegf* 5′mut and the control HCT116/YFP (Figure 3B). Furthermore, HCT116/*vegf* 5′ displayed a distinctive, anchorage-independent growth, while HCT116/*vegf* 5′mut and the control HCT116/YFP did not (Figure 3C and 3D).

Tumor-Forming Activity of the HCT116/*vegf* 5′ Clones

To demonstrate the malignancy of HCT116/*vegf* 5′ in vivo, athymic nude mice were injected subcutaneously with each clone, and growing tumor masses were measured. Both HCT116/*vegf* 5′mut and control HCT116/YFP formed small tumor masses that did not expand further (*vegf* 5′mut-tumor and YFP-tumor, respectively). In contrast, HCT116/*vegf* 5′ rapidly and progressively formed tumors (*vegf* 5′-tumor). The average volumes of the *vegf* 5′-tumors were 4-fold and 41-fold larger than those of the control YFP-tumors on days 5 and 28, respectively (Figure 4B). There was no significant difference between the sizes of tumors derived from *vegf* 5′-G3 clone and -G5 clone at either time point.

Histological examination showed that the growing *vegf* 5′-tumors contained central necrotic areas, while the *vegf* 5′mut-tumors formed a small nest of tumors encapsulated by connective tissue (Figure 4C). We next tested whether the accelerated growth of the *vegf* 5′-tumors was a consequence of enhanced proliferation, decreased apoptosis, or both. Apoptosis and proliferation were assessed by quantifying TUNEL-positive and BrdU-incorporating cells, respectively (Figure 4C). The *vegf* 5′-tumors showed a small, but significant increase in the numbers of BrdU-positive cells (Figure 4D) compared with the *vegf* 5′mut-tumors. The number of apoptotic cells in the *vegf* 5′-tumor was significantly lower than in the *vegf* 5′mut-tumor (Figure 4D). These results suggest that the *vegf* 5′UTR RNA may accelerate tumor growth by suppression of apoptosis and promotion of cell growth. We also examined the development of tumor vessels by staining with an Ab against an endothelial cell marker CD31. The *vegf* 5′-tumors significantly increased CD31-positive microvessels (Figure 4C) in association with enlargement of the tumors, compared with the *vegf* 5′mut-tumors.

Changes in Gene Expression in the *vegf* 5′-Tumors

Total RNA was prepared on day 14 from three different *vegf* 5′-tumors, and an equal amount of RNA from each tumor was mixed. Total RNA was also prepared from three different *vegf* 5′mut-tumors in the same manner. Using a microarray technique, gene expression profiles were compared between the two RNA samples. The *vegf* 5′-tumors up-regulated mRNA

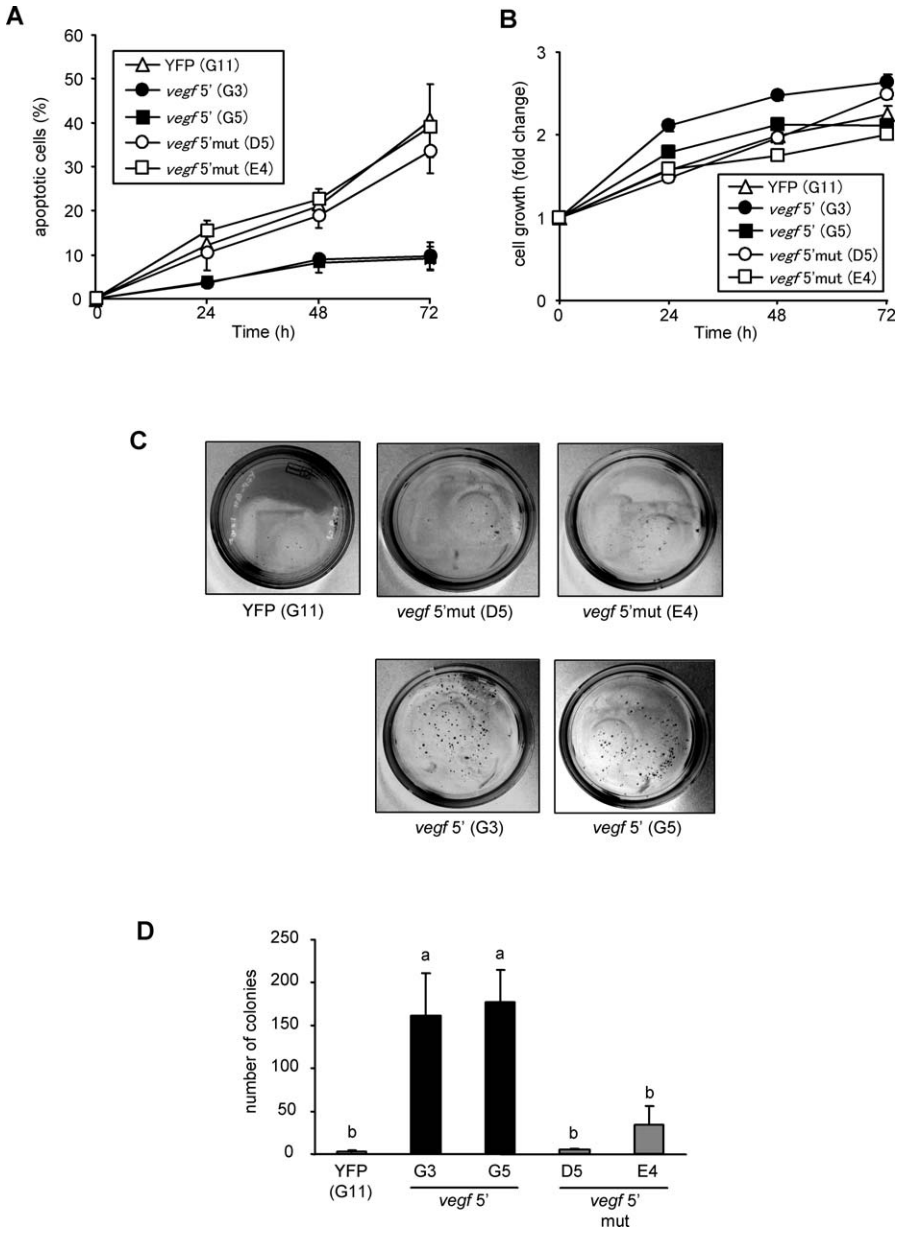

Figure 3. Characterization of HCT116 Cells Stably Expressing the *vegf* 5′UTR RNA

(A) 5-FU resistance in stable transfectant expressing the *vegf* 5′UTR RNA. Stably transfected HCT116 clones (HCT116/YFP-G11, HCT116/*vegf* 5′-G3, HCT116/*vegf* 5′-G5, HCT116/*vegf* 5′mut-D5, and HCT116/*vegf* 5′mut-E4) were treated with 80 μM 5-FU for the indicated time, and then apoptotic cells were identified and quantitated by the TUNEL-staining method. Values are means ± SEM from three independent experiments.

(B) Growth rate of the stable transfectants. Cell growth was assessed by MTT assay at the indicated time points. Results are expressed as relative increases in the absorbance, compared with that at time 0. Values are means ± SEM, $n = 4$.

(C and D) Increase in anchorage-independent growth ability in the *vegf* 5′UTR-expressing clones. The stably transfected clones were cultured in semi-solid medium for 28 d as described in the Methods. Pictures of growing colonies on day 28 are shown in (C), and the number of colonies were counted (D). Values are means ± SEM from three independent experiments. Means with different superscripts are significantly different by ANOVA followed by Scheffé's test ($p < 0.05$).

doi:10.1371/journal.pmed.0050094.g003

expression of 377 genes and down-regulated 295 genes >2-fold, compared with the *vegf* 5′mut-tumors (see gene lists in Tables S1 and S2). One of the distinctive identifying features of the listed genes was that the *vegf* 5′-tumors selectively down-regulated pro-apoptotic genes (eight genes) and up-regulated anti-apoptotic genes (five genes). Quantitative RT-PCR validated the significant up-regulation of an anti-apoptotic gene (*mia*) and down-regulation of pro-apoptotic genes (*fas*, *pcdc1*, *nrg1*, and *bax*) (Table 1).

It should also be noted that a major set of IFN-inducible genes (43 genes) were specifically down-regulated in the *vegf* 5′-tumors (Table 2), whereas none of IFN-inducible genes were included in the up-regulated genes (Table S1). Using quantitative RT-PCR, we compared mRNA levels of nine IFN-inducible genes between the *vegf* 5′-tumors and the *vegf* 5′mut-tumors, and validated significant down-regulation of eight out of nine genes in the *vegf* 5′-tumors (Table 1). An IFN-inducible gene *stat1* encoding a critical transcription

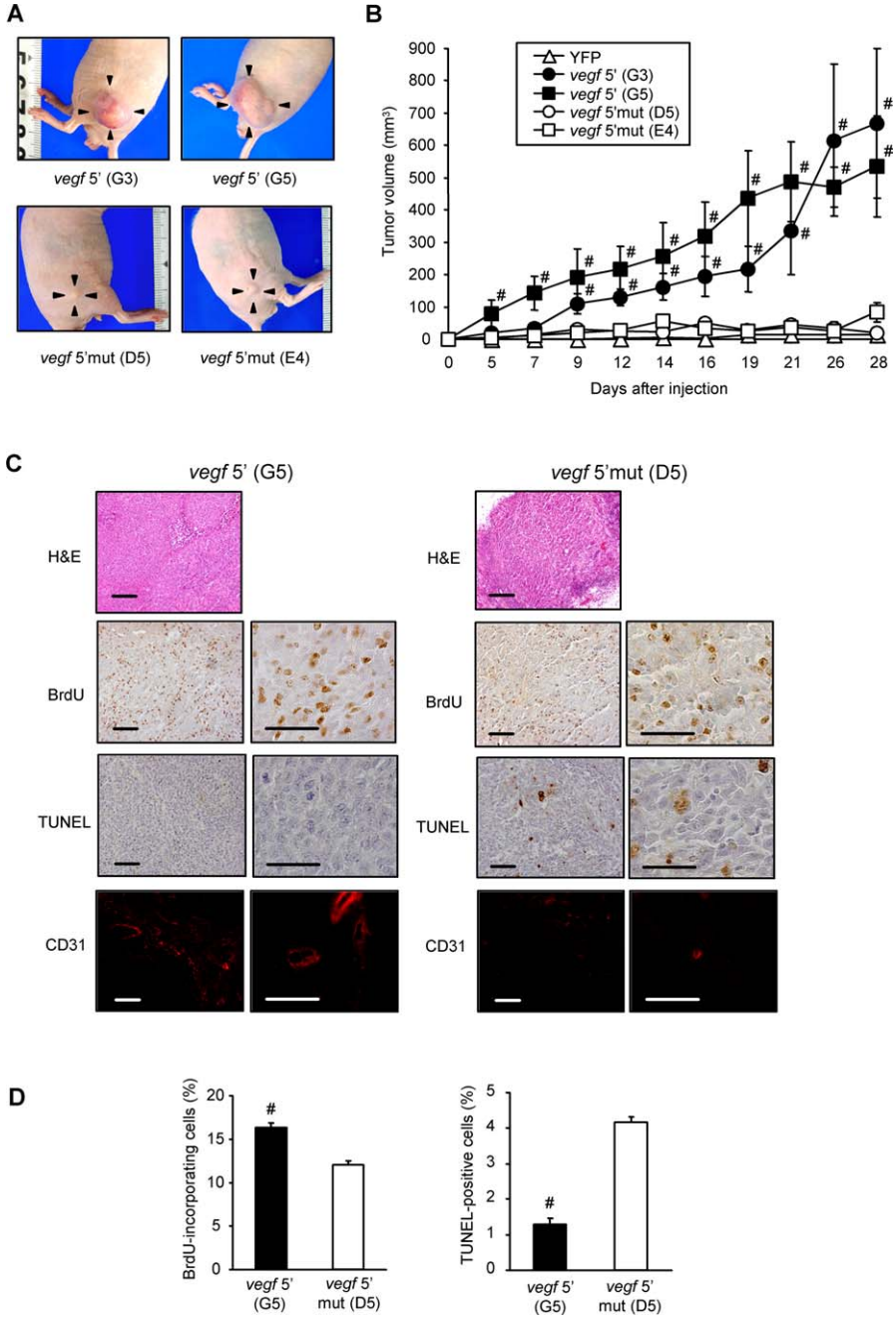

Figure 4. Tumor Formation of HCT116 Cells Stably Expressing the *vegf* 5′UTR RNA In Vivo

(A and B) In vivo tumorigenesis in xenografts of stable transfectants. Typical examples of growing tumors on day 28 are shown in (A). Tumor growth was assessed up to 28 d after inoculation, and tumor volume (mm^3) was calculated by the formula ($L \times W^2 \times 0.5$). Time-dependent changes in tumor masses are shown in (B). Values are means ± SEM from six independent experiments. There were no significant differences between *vegf* 5′-G3 and -G5 or among YFP-G11, *vegf* 5′mut-D5, and *vegf* 5′mut-E4 tumors. #, significantly different compared to YFP-G11, *vegf* 5′mut-D5, and *vegf* 5′mut-E4 tumors at each time point ($p < 0.05$ by ANOVA and Scheffé's test).

(C) Immunohistochemistry of the xenografts. On day 28 after inoculation, the growing tumors of *vegf* 5′-G3 and *vegf* 5′mut-D5 were subjected to hematoxylin and eosin (HE) staining, immunohistochemistry using a mouse monoclonal Ab against BrdU or CD31, or TUNEL staining. Bars indicate 100 μm in the left photograph in each panel, and 50 μm in the right photograph in each panel.

(D) Enhanced proliferation and suppressed apoptosis in the *vegf* 5′UTR-expressing tumors. Proliferation was assessed by calculating the percentages of BrdU-incorporating cells (left panel). Apoptosis was evaluated by calculating the percentages of TUNEL-positive cells (right panel). Values are means ± SEM from five independent experiments. #, Significantly different compared to *vegf* 5′mut-D5 tumors ($p < 0.05$ by two-tailed Student's *t*-test).

doi:10.1371/journal.pmed.0050094.g004

factor for both type I (α/β) and type II (γ) IFNs [33] was also significantly down-regulated, suggesting specific deactivation of the IFN/STAT1 pathway in the rapidly growing *vegf* 5′-tumors.

STAT1 Expression and Responsiveness to IFNs

To confirm that the *vegf* mRNA 5′UTR selectively deactivated the IFN-dependent pathway in vitro, we measured the levels of *stat1* mRNA and its protein in each stable clone by

Table 1. Validation of Microarray Data on Selected Genes by Quantitative RT-PCR

Type of Gene	Gene Symbol	Expression Ratio (/*gapdh*)		
		***vegf* 5′ (G5)**	***vegf* 5′mut (D5)**	***p*-Value**
Apoptosis-associated genes and growth factors	*MIA*	7.12 ± 0.25	2.92 ± 0.52	0.002
	BCL6	0.80 ± 0.08	0.61 ± 0.06	n.s.
	EGFR	1.39 ± 0.07	1.60 ± 0.09	n.s.
	NRG1	1.48 ± 0.44	14.21 ± 0.12	<0.001
	PCDC1	1.60 ± 1.47	2,136.54 ± 160.90	<0.001
	FAS	0.7 ± 0.11	2.01 ± 0.11	<0.001
	BAX	0.55 ± 0.07	1.04 ± 0.07	0.009
Interferon-responsive genes	*XAF1*	0.82 ± 0.02	10.49 ± 1.26	0.002
	TRAIL/Apo2L	5.24 ± 0.12	84.64 ± 14.42	0.005
	OAS1	3.42 ± 0.43	21.36 ± 2.24	0.001
	OAS2	0.01 ± 0.003	0.99 ± 0.22	0.012
	IRF1	0.82 ± 0.23	2.88 ± 0.63	0.037
	NMI	4.04 ± 1.16	22.68 ± 3.43	0.007
	ISG20	4.48 ± 0.58	23.59 ± 3.34	0.005
	PML	1.26 ± 0.32	4.12 ± 1.11	n.s.
	STAT1	18.51 ± 3.07	54.14 ± 6.07	0.005

Values are means ± SEM, $n = 3$. Significant difference ($p < 0.05$) based on two-tailed Student's *t*-test. n.s., not significant.
doi:10.1371/journal.pmed.0050094.t001

quantitative RT-PCR and immunoblotting, respectively. Similar amounts of *stat1* mRNA were observed among all clones (Figure 5A). Both HCT116/YFP and HCT116/*vegf* 5′mut cells responded to rhIFNα and up-regulated *stat1* mRNA expression, but this up-regulation was not observed in the HCT116/*vegf* 5′ clones (Figure 5A). Consistent with these, induction of STAT1 protein by IFNα was defect in the HCT116/*vegf* 5′cells (Figure 5B).

STAT1 plays a crucial role in the expression of the majority of IFN-inducible genes [34]. We therefore tested whether the HCT116/*vegf* 5′ cells actually showed decreased STAT1-dependent transcriptional activity. For this purpose, we used two different STAT1-dependent reporter plasmids encoding a promoter that either contained ISRE-binding sites (pISRE-Luc) that mainly respond to IFNα or GAS-binding sites (pGAS-Luc) that preferentially respond to IFNγ. Each stable clone was transiently transfected with pISRE-Luc or pGAS-Luc reporter plasmid, and then they were treated with rhIFNα or rhIFNγ for 24 h. In the HCT116/*vegf* 5′ clones, there was significant impairment of the IFNα-stimulated response of ISRE (Figure 5C) and the IFNγ-dependent response of GAS (Figure 5D) compared to the HCT116/*vegf* 5′mut clones or to the HCT116/YFP cells (Figure 5C and 5D). We confirmed that the IFN receptors were equally expressed in all clones tested (FigureS9A). These results suggest that the IFNα pathway might be more severely impaired than the IFNγ pathway. We also measured the levels of endogenous IFNα, β, and γ mRNAs in each clone by quantitative RT-PCR. There was no difference in the level of IFNα mRNA in each clone (Figure S9B). Neither clone expressed detectable amounts of IFNβ or IFNγ mRNAs.

We further examined the effects of stable knockdown of endogenous *vegf* mRNA on STAT1 expression in HCT116 cells (HCT116/siVEGF). Endogenous *vegf* mRNA was successfully silenced in the HCT116/siVEGF clones (Figure 6A). As shown in Figure 6B, the basal and the IFNα-stimulated expression levels of STAT1 were significantly increased in the HCT116/siVEGF clones compared with the control clone (HCT116/siControl) and parental cells (HCT116). Consistent with these results, both the basal and the IFNα-stimulated ISRE-dependent transcriptional activities were increased 2- to 3-fold in the HCT116/siVEGF clones (Figure 6C).

Impairment of the IFNα-Dependent Anti-apoptotic Pathway in Growing *vegf* 5′-Tumors

To assess whether the reduced IFN signals were responsible for the malignant transformation of the HCT116/*vegf* 5′ cells, we examined the effect of IFNs on 5-FU-induced apoptosis, as IFNs are known to potentiate the pharmacological action of 5-FU [35]. Treatment with rhIFNα or rhIFNγ alone did not induce apoptosis in any of the clones tested, while both IFNα and IFNγ significantly enhanced 5-FU-induced apoptosis in the HCT116/*vegf* 5′mut cells or the HCT116/YFP cells (Figure 5E and 5F). In contrast, neither IFNα nor IFNγ had an effect in the HCT116/*vegf* 5′ cells.

Finally, we examined whether growing *vegf* 5′-tumors had impaired responses to IFNα in vivo. We therefore focused on the effects of rhIFNα on tumor growth. For these experiments, we implanted HCT116/*vegf* 5′ (5×10^6 cells) in the left flank and either HCT116/YFP (1×10^7 cells) or HCT116/*vegf* 5′mut (1×10^7 cells) in the right flank of the same animal. When both tumors reached approximately 40 mm^3 on day 7, we started to treat the mouse once a day with 5-FU (30 mg/kg body weight) or with a combination of 5-FU (30 mg/kg body weight) and rhIFNα (50,000 U). At day 4 in the YFP-tumors (Figure 7A) or day3 in the *vegf* 5′mut-tumors (Figure 7C) after the 5-FU treatment, the YFP-tumors and the *vegf* 5′mut-tumors began to reduce in size, respectively. Simultaneous treatment with rhIFNα accelerated this reduction and most tumors disappeared within 7 d. In contrast, the responses of the *vegf* 5′-tumors to 5-FU and rhIFNα were strikingly different. Treatment with 5-FU initially and transiently decreased tumor sizes, but they then began to grow rapidly from day 4 (Figure 7B). Simultaneous administration of rhIFNα did not have any effect on tumor growth.

Table 2. List of IFN-Responsive Genes Selectively Down-Regulated in *vegf* 5′UTR-Overexpressing Cells

Gene Symbol	Genbank Accession Number	Gene Name	Fold Change
GBP1	NM_002053	Guanylate binding protein 1, interferon-inducible, 67 kDa	0.03
IFIT2	NM_001547	Interferon-induced protein with tetratricopeptide repeats 2	0.06
OASL	NM_003733	2′-5′-oligoadenylate synthetase-like	0.09
IL28A	NM_172138	Interleukin 28A (interferon, lambda 2)	0.1
XAF-1	NM_017523	XIAP associated factor-1	0.11
TRAIL/Apo2L	NM_003810	Tumor necrosis factor (ligand) superfamily, member 10	0.12
IL29	NM_172140	Interleukin 29 (interferon, lambda 1)	0.12
TLR3	NM_003265	Toll-like receptor 3	0.13
OAS2	NM_016817	2′-5′-oligoadenylate synthetase 2, 69/71 kDa	0.13
IFI44L	NM_006820	Interferon-induced protein 44-like	0.18
IFIT3	NM_001549	Interferon-induced protein with tetratricopeptide repeats 3	0.18
IFI44	NM_006417	Interferon-induced protein 44	0.19
IFIT1	NM_001548	Interferon-induced protein with tetratricopeptide repeats 1	0.19
IFI35	NM_005533	Interferon-induced protein 35	0.2
NMI	NM_004688	N-myc (and STAT) interactor	0.23
CD47	NM_198793	CD47 antigen	0.27
IFITM1	NM_003641	Interferon-induced transmembrane protein 1 (9–27)	0.28
FAS	NM_000043	Fas (TNF receptor superfamily, member 6)	0.29
ISG20	NM_002201	Interferon-stimulated exonuclease gene 20 kDa	0.29
OAS1	NM_002534	2′,5′-oligoadenylate synthetase 1, 40/46 kDa	0.32
IFI16	AK094968	Interferon, gamma-inducible protein 16	0.34
IFIH1	NM_022168	Interferon induced with helicase C domain 1	0.35
Galectin 9	NM_009587	Lectin, galactoside-binding, soluble, 9 (galectin 9)	0.35
THSD4	NM_024817	thrombospondin, type I, domain containing 4	0.37
IRF1	NM_002198	Interferon regulatory factor 1	0.37
PML	NM_033238	Promyelocytic leukemia	0.38
MYD88	NM_002468	Myeloid differentiation primary response gene (88)	0.39
IFITM2	NM_006435	Interferon-induced transmembrane protein 2 (1–8D)	0.4
TAP1	NM_000593	Transporter 1, ATP-binding cassette, sub-family B (MDR/TAP)	0.41
PLSCR1	NM_021105	Phospholipid scramblase 1	0.41
IFITM3	NM_021034	Interferon-induced transmembrane protein 3 (1–8U)	0.43
HLA-G	M90686	HLA-G histocompatibility antigen, class I, G	0.43
IFI6	NM_022873	Interferon, alpha-inducible protein 6	0.43
SP110	NM_004510	SP110 nuclear body protein	0.43
ISG20L1	NM_022767	Interferon-stimulated exonuclease gene 20 kDa-like 1	0.44
MMP2	NM_004530	Matrix metallopeptidase 2	0.46
C1R	NM_001733	Complement component 1, r subcomponent	0.46
IFIT5	NM_012420	Interferon-induced protein with tetratricopeptide repeats 5	0.47
HLA-C	BC008457	Major histocompatibility complex, class I, C	0.47
HLA-A	NM_002116	Major histocompatibility complex, class I, A	0.47
B2M	NM_004048	Beta-2-microglobulin	0.48
STAT1	NM_007315	Signal transducer and activator of transcription 1, 91 kDa	0.49
IFI30	NM_006332	Interferon, gamma-inducible protein 30	0.49

doi:10.1371/journal.pmed.0050094.t002

Discussion

In the present study, we show a novel function of the *vegf* 5′UTR in tumor cell survival and growth. Both treatment of *vegf*-knockdown HCT116 cells with rhVEGF$_{165}$ and treatment of VEGF$_{165}$-overexpressing HCT 116 cells with a neutralizing anti-VEGF$_{165}$ Ab suggest the presence of *vegf* mRNA-mediated anti-apoptotic action against anti-cancer drugs (5-FU, etoposide, and doxorubicin). We determined that the anti-apoptotic action resided in a 270-nt-long element between positions nt 475 and nt 745 of the 5′ UTR of *vegf* mRNA. The 5′ UTR could exert the anti-apoptotic action even in the presence of a protein synthesis inhibitor. These results suggest that the 5′UTR may function as a regulatory RNA.

To further clarify the potential role of *vegf* 5′UTR RNA, we established HCT116/*vegf* 5′ and HCT116/*vegf* 5′mut clones. HCT116/*vegf* 5′ cells, but not HCT116/*vegf* 5′mut cells, showed anchorage-independent growth in vitro and rapidly grew when implanted in athymic nude mice, indicating that *vegf* mRNA 5′UTR facilitates tumor progression. The rapid growth observed in the *vegf* 5′-tumors might be due to the acquisition of resistance to apoptosis (the process that eliminates defective cells), which contributes to tumor development and resistance to drug therapy. Microarray and quantitative RT-PCR analyses demonstrated that expression of pro-apoptotic genes (*fas*, *pdcd1*, *nrg1*, and *bax*) and an anti-apoptotic gene (*mia*) was up-regulated and markedly down-regulated, respectively, in the rapidly growing *vegf* 5′-tumors. In addition, microarray analysis also showed that the expression of cell growth-promoting genes (*cxcl1*, *cxcl2*, *cxcr4*, *mia1*, and *fgf-19*) was up-regulated in the rapidly growing *vegf* 5′-tumors.

The combination of both dysregulated cell proliferation and suppressed cell death are required for neoplastic progression [36]. In addition, survival and growth under

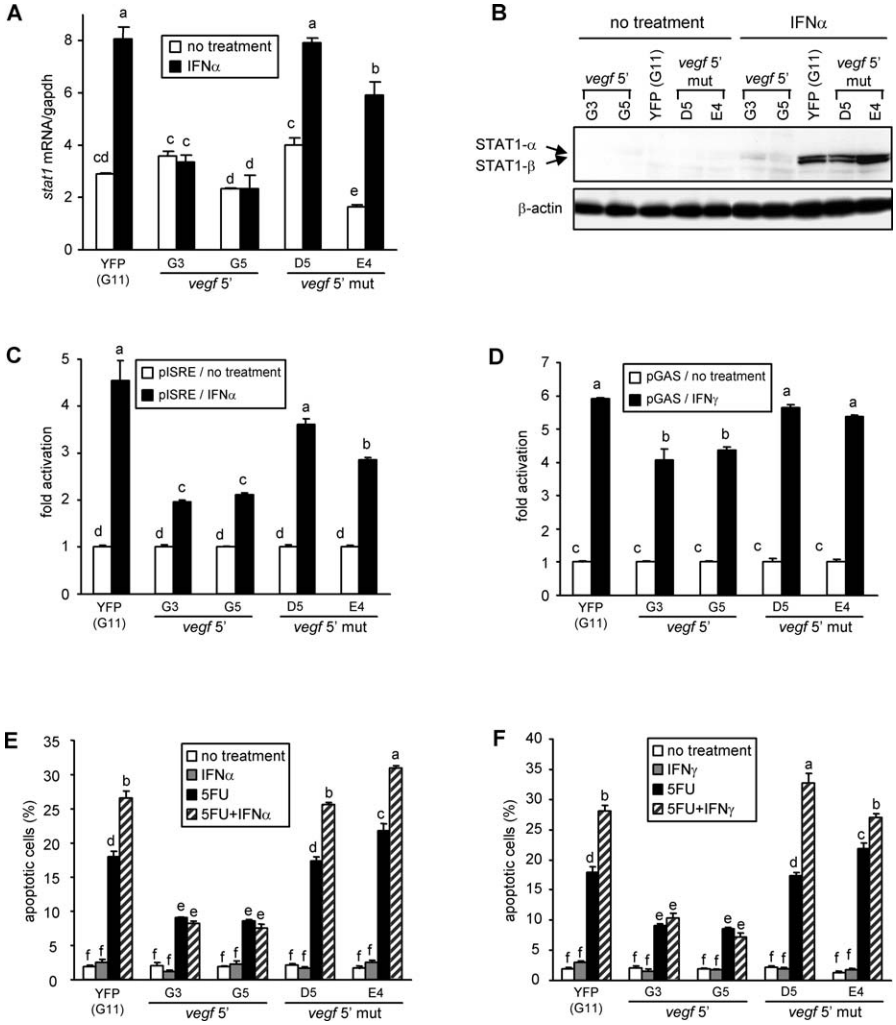

Figure 5. Impaired Responses to IFNs in the *vegf* 5′UTR-Expressing Clones

(A and B) Repression of *stat1* mRNA and its protein expression in the *vegf* 5′UTR-expressing cells. Total RNA or whole cell extracts were prepared from the indicated clones before and 24 h after treatment with 500 U/ml rhIFNα. Levels of *stat1* mRNA were measured using quantitative RT-PCR (A). Values were normalized for the amount of *gapdh* mRNA (means ± SEM, $n = 4$). Means with different superscripts are significantly different by ANOVA and Scheffé's test ($p < 0.05$). Amounts of STAT1α (91 kDa) and STAT1β (84 kDa) isoforms were measured by Western blot analysis using an anti-STAT1 Ab (B, upper panel). The levels of β-actin are shown as a loading control (B, lower panel).

(C and D) Suppression of IFN-mediated transactivation activities in the *vegf* 5′UTR-expressing cells. Each stable transfectant was transiently cotransfected with pTK-*Renilla* (as a monitor for transfection efficiency) and with a luciferase reporter plasmid containing ISRE sequence (C) or GAS sequence (D). Twenty-four hours after transfection, the cells were treated with 500 U/ml rhIFNα (C) or 500 U/ml rhIFNγ (D) for 24 h. The luciferase activity of each construct was calculated as LucF/LucR activity. Results are expressed as fold changes compared to untreated cells. Means with different superscripts are significantly different by ANOVA and Scheffé's test ($p < 0.05$).

(E) Resistance to 5-FU and IFNα in the *vegf* 5′UTR-expressing cells. Stable transfectants were untreated or treated with 500 U/ml rhIFNα, 80 μM 5-FU, or 80 μM 5-FU plus 500 U/ml rhIFNα for 48 h. Percentages of apoptotic cells were calculated by the TUNEL-staining method. Values are means ± SEM, $n = 4$. Means with different superscripts are significantly different by ANOVA and Scheffé's test ($p < 0.05$).

(F) Resistance to 5-FU and IFNγ in the *vegf* 5′UTR-expressing cells. As in (E), but 500 U/ml rhIFNγ was used instead of 500 U/ml rhIFNα. Values are means ± SEM, $n = 4$. Means with different superscripts are significantly different by ANOVA and Scheffé's test ($p < 0.05$).

doi:10.1371/journal.pmed.0050094.g005

anchorage-independent conditions are required for the progression [37]. This anchorage-independent property of tumor cells correlates with their in vivo oncogenic potential. Thus, we consider that the *vegf* 5′UTR may increase the ability not only to suppress apoptosis but also to survive and grow in an anchorage-independent manner, resulting in the acceleration of tumor formation.

The precise sequence and structure of the 5′UTR of *vegf* mRNA as well as the molecular target(s) that interact with the RNA remain to be elucidated. However, it seems likely that such a profound change in cell function induced by RNA would require a global change of gene expression in cells. Our results support this notion by showing that the *vegf* mRNA 5′UTR modulated expression of numerous genes. One of the striking findings is that many of the down-regulated genes belong to a set of IFN-inducible genes, including *stat1*.

Since it is reported that IFN down-regulates IRES-dependent translation of distinct mRNAs [38], overexpression of the IRES-containing 5′UTR might attenuate the IFN signal, leading to the down-regulation of IFN-inducible genes. We therefore tested whether IFNα affected IRES activity of *c-myc*, *fgf-2*, or *bip* using a bicistronic luciferase assay system (Figure

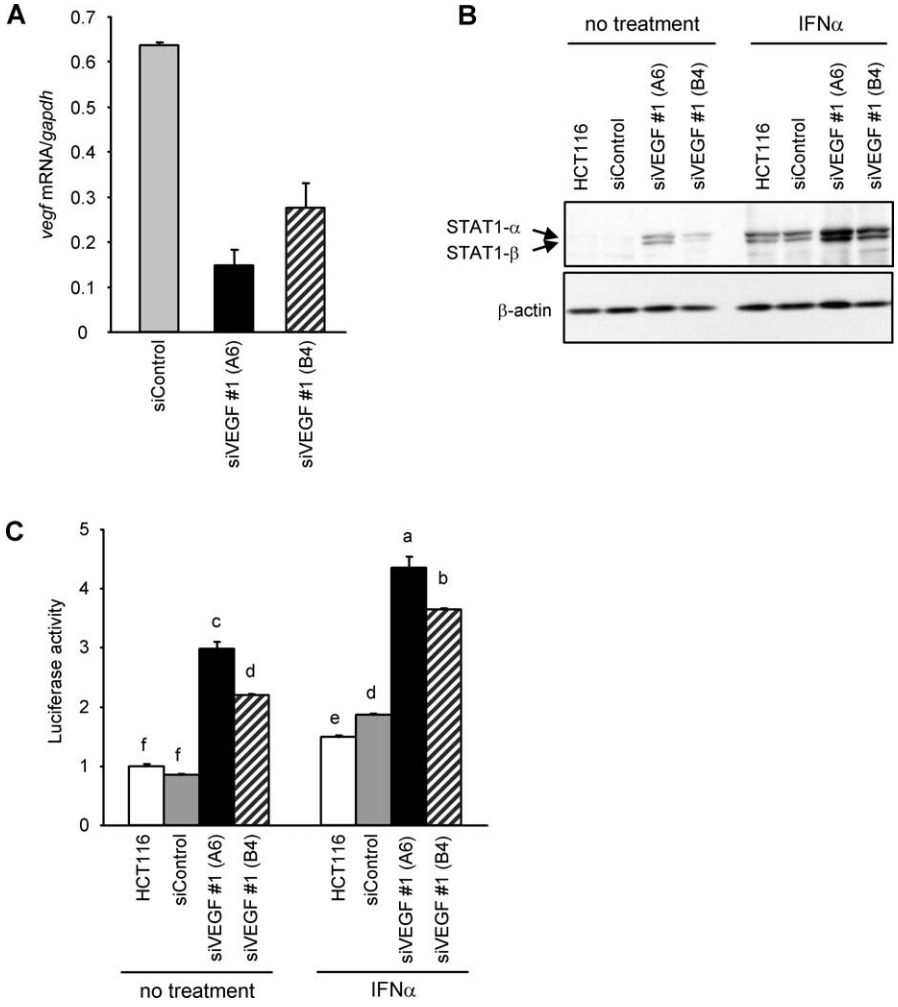

Figure 6. Enhancement of STAT1 Expression and IFNα Response in the Stable *vegf* Knockdown Cells

(A) Expression levels of *vegf* mRNA were measured using quantitative RT-PCR. Values were normalized for the amount of *gapdh* mRNA (means ± SEM, $n = 4$).

(B) Increased expression of STAT1 in the stable *vegf* knockdown cells. Total proteins were extracted from the indicated clones before and 24 h after treatment without or with 500 U/ml IFNα. Amounts of STAT1α and STAT1β isoforms were measured by Western blot analysis using an anti-STAT1 Ab.

(C) Enhancement of IFNα-mediated transactivation activity in the stable *vegf* knockdown cells. Each stable transfectant was transiently cotransfected with pISRE reporter plasmid and pTK-*Renilla*. Twenty-four hours after transfection, the cells were treated without or with 500 U/ml rhIFNα for 24 h. The luciferase activity of each construct was calculated as firefly luciferase/*Renilla* luciferase activity. Means with different superscripts are significantly different by ANOVA and Scheffé's test ($p < 0.05$).

doi:10.1371/journal.pmed.0050094.g006

S7A) in our experimental conditions, and found that IFNα did not modify at least these IRES activities (Figure S7C). At the same time, we also confirmed that IFNα signaling, estimated using the ISRE-dependent transcription reporter assay, was not inhibited in the cells overexpressing *bip*, *c-myc*, or *fgf-2* 5′UTR, nor was it inhibited in the cells overexpressing the *pdgf-b* 5′UTR that have no IRES activity (Figure S7D). Although these results suggest that the suppression of IFN signaling may be specific for the *vegf* 5′UTR, further studies are needed to clarify the molecular mechanism for the suppression.

The IFNs/STAT1 signal is one of the key pathways for tumor suppression. Mice with a targeted deletion of the STAT1 or IFNγ receptor develop chemically induced or spontaneous tumors more rapidly than wild-type mice [39]. Similarly, mouse embryonic fibroblasts deficient in the IFNα receptor undergo spontaneous malignant transformation, and the IFNα receptor-deficient mice develop papillomas of the skin at a high rate when treated with a chemical carcinogen [40]. In contrast, the reconstitution of STAT1 suppressed the tumorigenicity of STAT1-deficient tumor cells in vivo, demonstrating that STAT1 acts as an important tumor suppressor [41]. Indeed, the majority of cancer cell lines and primary tumors are resistant to IFNs, often through inhibition of STAT1 expression [42,43]. We propose here that the *vegf* mRNA 5′UTR negatively regulates expression of STAT1, leading to suppression of STAT1-dependent transcriptional activities. It has been suggested that STAT1 directly regulates DNA damage-induced apoptosis by transcriptional activation of apoptosis modulating genes, such as TRAIL, Fas, and XAF-1 [33], all of which were down-regulated in the *vegf* 5′-tumors (Table 1). Thus, the suppression of STAT1 may be crucial for malignant transformation of

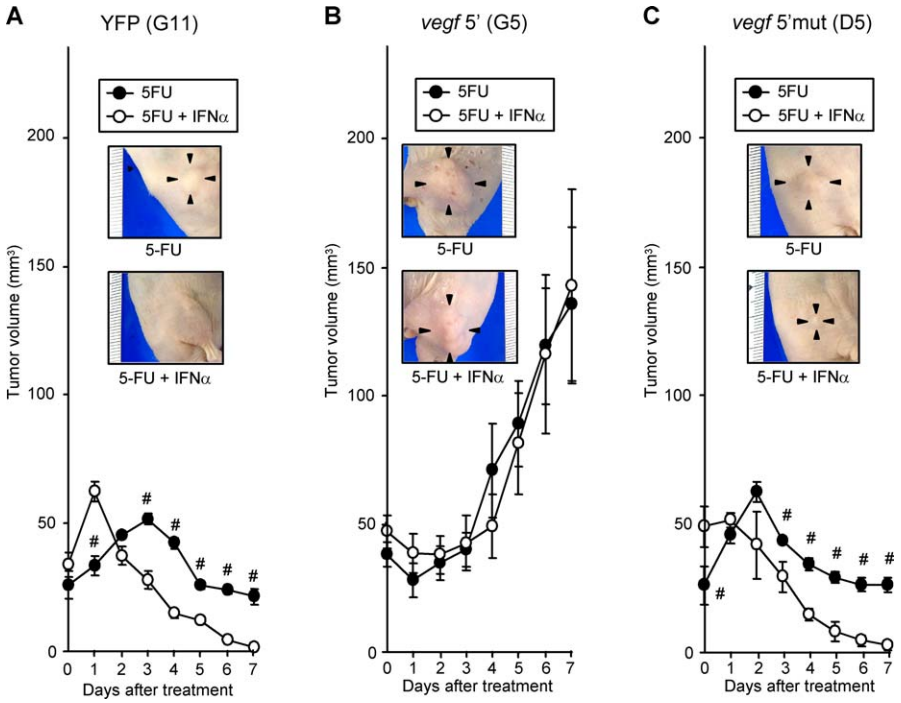

Figure 7. Effects of IFNα Treatment on Growth of Xenograft Tumors

An athymic nude mouse was implanted subcutaneously with the *vegf* 5′-G5 clone (5×10^6 cells) in the right flank (B) and the YFP-G11(A) or the *vegf* 5′mut-D5 clone (C) (1×10^7 cells) in the left flank. On day 7 when tumors had grown to be palpable, the mouse was intraperitoneally injected with 5-FU (30 mg/kg body weight), or 5-FU (30 mg/kg body weight) plus rhIFNα (50,000 U) once a day. Time-dependent changes in tumor masses were measured as described in the legend to Figure 4. Values are means ± SEM, $n = 4$. #, Significantly different compared to 5-FU-treated tumors at each time point ($p < 0.05$ by two-tailed Student's *t*-test). A photograph showing a typical tumor growing on day 7 of IFN-treatment is inserted in each figure.

doi:10.1371/journal.pmed.0050094.g007

HCT116/*vegf* 5′ cells. In fact, the *vegf* 5′-tumors did not response to IFNα therapy (Figure 7).

Tumor cell growth and survival may require both expression of VEGF and down-regulation of the IFN pathway. Consistent with this notion, it is known that IFNα transcriptionally suppresses VEGF expression [44,45]. In contrast, we suggest here that *vegf* mRNA may negatively regulate the IFN signaling pathway by repressing STAT1. This reciprocal regulation of VEGF and STAT1 is entirely feasible as these two molecules exert opposing biological functions: VEGF promotes proliferation, metastasis, and angiogenesis [1–4], and inhibits apoptosis [1]; in contrast, STAT1 negatively regulates proliferation, metastasis, and angiogenesis [41,46], and promotes apoptosis [33,47]. Tumor cells abundantly expressing *vegf* mRNA [1,48,49] may use this negative regulatory mechanism to gain advantages of growth and survival to escape from the IFN-mediated anti-tumor machinery. Indeed, we found here that stable knockdown of endogenous *vegf* mRNA by siRNA increased STAT1 expression.

At present, the precise mechanisms for the *vegf* 5′UTR-mediated anti-apoptotic action are still unknown. However, our preliminary experiments showed that the *vegf* 5′UTR RNA might interact with double-stranded RNA-activated protein kinase (PKR) protein in the cells expressing the full-length *vegf* mRNA or the *vegf* 5′UTR RNA, which were examined by the pull-down assay using an antisense oligonucleotide probe specific for the *vegf* 5′UTR sequence (unpublished data). It is reported that PKR binds several structured UTRs of mRNA, such as the 5′UTR of *ifn-γ* mRNA [50], the 3′UTR of *α-tropomyosin* mRNA [51], and the 3′UTR of *tnf-α* mRNA [52]. PKR associates with tumor suppressor, such as IRF-1 and p53 [53] and induces apoptosis. Our preliminary data suggest that the *vegf* 5′UTR might interact with PKR and lead to suppression of PKR-mediated apoptotic pathway. However, this is still an unproven hypothesis, and further experiments are being carried out in our laboratory.

Recent studies have revealed that a large number of non-coding RNAs play a critical role in tumorigenesis [17]. Our findings support the concept originally put forward by Blau and colleagues [18,54] that non-coding regions of mRNAs can act as RNA regulators for tumor malignancy. There is increasing evidence that the UTR of certain mRNAs significantly suppresses the tumorigenic properties of cancer cells both in vitro and in vivo. The 3′UTR of *α-tropomyosin* mRNA suppresses the proliferation, invasion, and destruction of muscle tissues characteristic of rhabdomyosarcoma cells [18]. The 3′UTR of *ribonucleotide reductase*, a key rate-limiting enzyme in DNA synthesis, and the 3′UTR of *prohibitin*, an inhibitor of cell proliferation, significantly suppress the tumorigenic properties and metastatic phenotype of transformed fibroblasts and MCF7 cells [19,20]. In addition, the 5′UTR of the human *c-myc* P0 transcript suppresses the malignant phenotype of human breast cancer cells with decreased anchorage-independent proliferation, enhanced susceptibility to programmed cell death, and complete loss of the ability to form tumors in the intact animal [21]. To the

best of our knowledge, the 5′UTR *vegf* mRNA is the first example of tumor-promoting UTR RNA.

VEGF protein is considered to be an important therapeutic target for cancer treatment, and anti-VEGF strategies are undergoing clinical evaluation [14]. A number of preclinical studies have demonstrated that anti-VEGF therapy alone can suppress the growth of established tumors [55,56]. Unlike these preclinical studies, anti-VEGF-specific Ab (bevacizumab) alone has not been shown to increase survival in lung and colorectal cancer patients [14]. The combined use of bevacizumab with standard chemotherapy increased overall survival in metastatic colorectal cancer [57], but did not improve the clinical outcome in metastatic breast cancers in previously treated patients [58]. Furthermore, the combination of the VEGF receptor tyrosine kinase inhibitor, vatalanib, with chemotherapy did not show an increased survival rate in metastatic colorectal cancer patients [59]. Our finding that the novel intrinsic tumor-promoting activity presents in the *vegf* mRNA might explain, at least in part, the inconsistencies of outcome associated with VEGF-VEGFR strategies. The present study suggests that both *vegf* mRNA and VEGF protein may synergistically promote the malignancy of tumor cells. Thus anti-*vegf* transcript therapy, such as siRNA-based gene silencing, in combination with anti-VEGF therapy might provide optimal anti-tumor effects, including inhibition of angiogenesis, blockade of tumor cell survival, and enhanced sensitivity to radiation and drug therapies.

Supporting Information

Figure S1. Effect of *vegf* Transcript on Susceptibility to Anti-cancer Drugs

(A and B) Knockdown of *vegf* transcript increases apoptosis induced by etoposide and doxorubicin. Cells untransfected (–) or transfected with the indicated plasmids for 24 h were treated with 3 μM etoposide (A), 20 nM doxorubicin (B), or rhVEGF protein (1 or 2 ng/ml) combined with each drug for 40 h. Apoptosis was evaluated by calculating the percentages of TUNEL-positive cells. Values are means ± standard error of the mean (SEM) from four independent experiments. Means with different superscripts are significantly different by ANOVA followed by Scheffé's test ($p < 0.05$).
(C and D) Overexpression of *vegf* transcript induces resistance to anti-cancer drugs. Cells untransfected (–) or transfected with the indicated constructs for 24 h were treated with 20 μM etoposide (C) or 340 nM doxorubicin (D) for 48 h, and then apoptosis was evaluated by the TUNEL method. Values are means ± SEM from three independent experiments. Means with different superscripts are significantly different by ANOVA followed by Scheffé's test ($p < 0.05$).

Found at doi:10.1371/journal.pmed.0050094.sg001 (1.1 MB TIF)

Figure S2. Expression of Transfected Construct Transcripts and Their Proteins

(A) Levels of transfected *vegf* mRNAs and their proteins were measured by Northern and Western analyses, respectively. Northern hybridization of *vegf* mRNA was performed using a cDNA probe specific for *vegf* ORF. Levels of HA-tagged VEGF and β-actin proteins were measured using a rabbit polyclonal anti-HA Ab and a mouse monoclonal Ab against β-actin, respectively.
(B) Levels of transfected *vegf* 5′UTR-CAT constructs were analyzed by Northern blot analysis using a cDNA probe specific for *cat*. Levels of L-VEGF protein were measured by Western blotting using a rabbit polyclonal anti-L-VEGF Ab.

Found at doi:10.1371/journal.pmed.0050094.sg002 (1.8 MB TIF)

Figure S3. Effects of *vegf* 5′UTR on 5-FU-Induced Apoptosis

(A–C) HCT116 cells transfected with the indicated plasmids for 24 h were treated with 80 μM 5-FU for 40 h. Cells undergoing apoptosis were detected by the TUNEL method (A and B) or the APOPercentage assay (C). Values are means ± SEM, $n = 4$. Means with different superscripts are significantly different by ANOVA and Scheffé's test ($p < 0.05$).
(D) Twenty-four hours after transfection with the indicated plasmids, the cells were treated with 80 μM of 5-FU or 80 μM 5-FU plus 5 μg/ml of the monoclonal mouse anti-human $VEGF_{165}$-neutralizing Ab (+ Ab) for 24 h. Then, apoptosis was evaluated by the caspase 3/7 activity. Means with different superscripts are significantly different by ANOVA followed by Scheffé's test ($p < 0.05$). *vegf* mRNA wt, wild-type full-length $vegf_{165}$ mRNA without mutation in sequence encoding signal peptide.

Found at doi:10.1371/journal.pmed.0050094.sg003 (5.5 MB TIF)

Figure S4. Effects of Several 5′UTR RNAs on Resistance to 5-FU in HCT116 Cells

Cells transfected with the indicated plasmid for 24 h were treated with 80 μM 5-FU for 40 h. Percentages of apoptotic cells were calculated. Values are means ± SEM, $n = 4$. Means with different superscripts are significantly different by ANOVA and Scheffé's test ($p < 0.05$).

Found at doi:10.1371/journal.pmed.0050094.sg004 (919 KB TIF)

Figure S5. Prediction of RNA Secondary Structures

The sequences of *vegf* 5′UTR (A) and mutated *vegf* 5′UTR (B) were analyzed using the mfold algorithm 3.2 of Zuker.
A circle shown in (A) indicates the stem-loop located in the region that is required for the *vegf* 5′UTR function.

Found at doi:10.1371/journal.pmed.0050094.sg005 (2.6 MB TIF)

Figure S6. Effects of *vegf* 5′UTR RNA on Resistance to 5-FU in RKO, HEK293, and AGS Cells

(A) The levels of mRNAs for VEGF receptors (*vegfr1*, *vegfr2*, *nrp1*, and *nrp2*) in the indicated cell lines were analyzed by RT-PCR.
(B–D) RKO cells (B), HEK293 cells (C), and AGS cells (D) were transfected with the indicated constructs for 24 h. The cells were untreated or treated with 150 μM 5-FU for 48 h. In the case of cells transfected with the plasmid expressing full-length *vegf* mRNA, the cells were treated with 150 μM 5-FU plus 5 μg/ml of a monoclonal anti-human $VEGF_{165}$-neutralizing Ab (+ Ab) for 48 h. Then, apoptosis was evaluated by the TUNEL method. Values are means ± SEM from three independent experiments. Means with different superscripts are significantly different by ANOVA followed by Scheffé's test ($p < 0.05$).

Found at doi:10.1371/journal.pmed.0050094.sg006 (1.4 MB TIF)

Figure S7. Effect of the *vegf* 5′UTR RNA or IFNα on Cellular IRES Activities

(A) Schematic diagram of bicistronic plasmid. The bicistronic cassette expresses the LucR in a cap-dependent manner and LucF in an IRES-dependent manner. Each IRES or hairpin control is located between the two cistrons.
(B) HCT116 cells were cotransfected with 0.5 μg of the indicated *vegf* 5′UTR-expressing plasmid and 0.25 μg of bicistronic plasmid containing the indicated 5′UTR. The each IRES activity was calculated as LucF/LucR activity.
(C) IFNα has no effect on cellular IRES activity. HCT116 cells were transfected with the indicated bicistronic plasmid for 24 h, then they were treated with 500 U/ml IFNα for 24 h. The luciferase activity of each construct was calculated as described in (B).
(D) Overexpression of IRES-containing 5′UTR has no effect on IFNα signaling. HCT116 cells were cotransfected with the indicated 5′UTR-CAT-expressing plasmid and luciferase reporter plasmid containing ISRE sequence. Twenty-four hours after transfection, the cells were treated with 500 U/ml rhIFNα for 24 h. The luciferase activity of each construct was measured and calculated as LucF/LucR activity.

Found at doi:10.1371/journal.pmed.0050094.sg007 (994 KB TIF)

Figure S8. Expression Levels of Transfected mRNA and Endogenous *vegf* mRNA, and Secretion Levels of VEGF by Stable Transfectants

(A) Levels of exogenous *vegf* 5′ UTR-*yfp* mRNA (upper panel), endogenous *vegf* mRNA (middle panel), and *gapdh* mRNA (loading control, lower panel) were measured by Northern hybridization using probes specific for *yfp*, *vegf* ORF, and *gapdh*, respectively. The transfectants expressed similar levels of chimeric RNA. The stable transfections of different chimeric mRNAs did not significantly changes the expression of endogenous *vegf* mRNA.
(B) Amounts of $VEGF_{165}$ secreted into the culture medium for 24 h were measured by ELISA assay. Values are means ± SEM, $n = 4$.

Found at doi:10.1371/journal.pmed.0050094.sg008 (1.5 MB TIF)

Figure S9. Expression of IFN Receptors and IFN-α2 mRNAs in Stable Clones

(A) The mRNA levels of IFN receptors (*ifnar1*, *ifnar2*, *ifngr1*, and *ifngr2*) and β-actin in the transfectants were measured by RT-PCR. Each stable clone showed similar levels of expression of *ifnr* mRNAs.
(B) The levels of *ifna2* mRNA in each clone were measured by quantitative RT-PCR.

Found at doi:10.1371/journal.pmed.0050094.sg009 (1.6 MB TIF)

Figure S10. Confirmation of the Specificity of Antibody Reactivity

Cell extracts were prepared from HCT116 cells treated with 500 U/ml IFN-α (A), or transfected with plasmid expressing L-VEGF (B), or HA-tagged VEGF (C). After each extract was either untreated (–) or treated (+) with antigen peptide, as described in the Methods section, they were subjected to Western blotting.

Found at doi:10.1371/journal.pmed.0050094.sg010 (1.1 MB TIF)

Table S1. List of All Genes Selectively Up-regulated in *vegf* 5′UTR-Expressing Tumors

Found at doi:10.1371/journal.pmed.0050094.st001 (462 KB DOC)

Table S2. List of All Genes Selectively Down-regulated in *vegf* 5′UTR-Expressing Tumors

Found at doi:10.1371/journal.pmed.0050094.st002 (365 KB DOC)

Accession Numbers

The GenBank (http://www.ncbi.nlm.nih.gov/) accession numbers of the genes discussed in this paper are *vegf-a* (NM__001025368), *mia* (NM__006533), *bcl6* (NM__138931), *egfr* (X00588), *nrg1* (NM__013962), *pdcd1* (NM__005018), *fas* (NM__000043), and *bax* (NM__138764).

The Gene Expression Omnibus (GEO) (http://www.ncbi.nlm.nih.gov/geo/) raw chip data files discussed in this paper are accession number GSE8888.

Acknowledgments

We thank Dr. Hervé Prats and Dr. Anne-Catherine Prats (INSERM U858, France) for providing polyclonal anti-L-VEGF Ab and plasmids (p165mSPHA3′, p165mSPHA, pVC, pSCT-CAT, pFGF2-CAT, pMycP2-CAT, pBip-CAT, pPDGFb-CAT, pRFL, pRMy2L, and pRBL).

Author contributions. KM, ST-K, and KR designed the research. KM, ST-K, MM, NY, YN, KN, and TK performed the research. KM and ST-K analyzed the data. KM, ST-K, and KR wrote the paper. KM, ST-K, MM, NY, YN, KN, TK, and KR discussed the results and commented on the manuscript.

References

1. Ferrara N, Davis-Smyth T (1997) The biology of vascular endothelial growth factor. Endocr Rev 18: 4–25.
2. Dvorak HF (2002) Vascular permeability factor/vascular endothelial growth factor: a critical cytokine in tumor angiogenesis and a potential target for diagnosis and therapy. J Clin Oncol 20: 4368–4380.
3. Hicklin DJ, Ellis LM (2005) Role of the vascular endothelial growth factor pathway in tumor growth and angiogenesis. J Clin Oncol 23: 1011–1027.
4. Bergers G, Benjamin LE (2003) Tumorigenesis and the angiogenic switch. Nat Rev Cancer 3: 401–410.
5. Zebrowski BK, Yano S, Liu W, Shaheen RM, Hicklin DJ, et al. (1999) Vascular endothelial growth factor levels and induction of permeability in malignant pleural effusions. Clin Cancer Res 5: 3364–3368.
6. Zebrowski BK, Liu W, Ramirez K, Akagi Y, Mills GB, et al. (1999) Markedly elevated levels of vascular endothelial growth factor in malignant ascites. Ann Surg Oncol 6: 373–378.
7. Hazelton D, Nicosia RF, Nicosia SV (1999) Vascular endothelial growth factor levels in ovarian cyst fluid correlate with malignancy. Clin Cancer Res 5: 823–829.
8. Minagawa N, Nakayama Y, Hirata K, Onitsuka K, Inoue Y, et al. (2002) Correlation of plasma level and immunohistochemical expression of vascular endothelial growth factor in patients with advanced colorectal cancer. Anticancer Res 22: 2957–2963.
9. Chao C, Al-Saleem T, Brooks JJ, Rogatko A, Kraybill WG, et al. (2001) Vascular endothelial growth factor and soft tissue sarcomas: tumor expression correlates with grade. Ann Surg Oncol 8: 260–267.
10. Lamszus K, Lengler U, Schmidt NO, Stavrou D, Ergun S, et al. (2000) Vascular endothelial growth factor, hepatocyte growth factor/scatter factor, basic fibroblast growth factor, and placenta growth factor in human meningiomas and their relation to angiogenesis and malignancy. Neurosurgery 46: 938–947; discussion 947–948.
11. Lissoni P, Rovelli F, Malugani F, Brivio F, Fumagalli L, et al. (2003) Changes in circulating VEGF levels in relation to clinical response during chemotherapy for metastatic cancer. Int J Biol Markers 18: 152–155.
12. Vincenzi B, Santini D, Russo A, Gavasci M, Battistoni F, et al. (2007) Circulating VEGF reduction, response and outcome in advanced colorectal cancer patients treated with cetuximab plus irinotecan. Pharmacogenomics 8: 319–327.
13. Byrne AM, Bouchier-Hayes DJ, Harmey JH (2005) Angiogenic and cell survival functions of vascular endothelial growth factor (VEGF). J Cell Mol Med 9: 777–794.
14. Jain RK, Duda DG, Clark JW, Loeffler JS (2006) Lessons from phase III clinical trials on anti-VEGF therapy for cancer. Nat Clin Pract Oncol 3: 24–40.
15. Sandler AB, Johnson DH, Herbst RS (2004) Anti-vascular endothelial growth factor monoclonals in non-small cell lung cancer. Clin Cancer Res 10: 4258s–4262s.
16. Lee TH, Seng S, Sekine M, Hinton C, Fu Y, et al. (2007) Vascular endothelial growth factor mediates intracrine survival in human breast carcinoma cells through internally expressed VEGFR1/FLT1. PLoS Med 4: e186. doi: 10.1371/journal.pmed.0040186
17. Costa FF (2005) Non-coding RNAs: new players in eukaryotic biology. Gene 357: 83–94.
18. Rastinejad F, Conboy MJ, Rando TA, Blau HM (1993) Tumor suppression by RNA from the 3′ untranslated region of alpha-tropomyosin. Cell 75: 1107–1117.
19. Manjeshwar S, Branam DE, Lerner MR, Brackett DJ, Jupe ER (2003) Tumor suppression by the prohibitin gene 3′untranslated region RNA in human breast cancer. Cancer Res 63: 5251–5256.
20. Fan H, Villegas C, Huang A, Wright JA (1996) Suppression of malignancy by the 3′ untranslated regions of ribonucleotide reductase R1 and R2 messenger RNAs. Cancer Res 56: 4366–4369.
21. Blume SW, Miller DM, Guarcello V, Shrestha K, Meng Z, et al. (2003) Inhibition of tumorigenicity by the 5′-untranslated RNA of the human c-myc P0 transcript. Exp Cell Res 288: 131–142.
22. Huez I, Creancier L, Audigier S, Gensac MC, Prats AC, et al. (1998) Two independent internal ribosome entry sites are involved in translation initiation of vascular endothelial growth factor mRNA. Mol Cell Biol 18: 6178–6190.
23. Akiri G, Nahari D, Finkelstein Y, Le SY, Elroy-Stein O, et al. (1998) Regulation of vascular endothelial growth factor (VEGF) expression is mediated by internal initiation of translation and alternative initiation of transcription. Oncogene 17: 227–236.
24. Huez I, Bornes S, Bresson D, Creancier L, Prats H (2001) New vascular endothelial growth factor isoform generated by internal ribosome entry site-driven CUG translation initiation. Mol Endocrinol 15: 2197–2210.
25. Teshima-Kondo S, Kondo K, Prado-Lourenco L, Gonzalez-Herrera IG, Rokutan K, et al. (2004) Hyperglycemia upregulates translation of the fibroblast growth factor 2 mRNA in mouse aorta via internal ribosome entry site. FASEB J: 03–1118fje.
26. Bornes S, Boulard M, Hieblot C, Zanibellato C, Iacovoni JS, et al. (2004) Control of the vascular endothelial growth factor internal ribosome entry site (IRES) activity and translation initiation by alternatively spliced coding sequences. J Biol Chem 279: 18717–18726.
27. Martineau Y, Le Bec C, Monbrun L, Allo V, Chiu IM, et al. (2004) Internal ribosome entry site structural motifs conserved among mammalian fibroblast growth factor 1 alternatively spliced mRNAs. Mol Cell Biol 24: 7622–7635.
28. Zuker M (2003) Mfold web server for nucleic acid folding and hybridization prediction. Nucl Acids Res 31: 3406–3415.
29. Kawahara T, Kuwano Y, Teshima-Kondo S, Takeya R, Sumimoto H, et al. (2004) Role of nicotinamide adenine dinucleotide phosphate oxidase 1 in oxidative burst response to Toll-like receptor 5 signaling in large intestinal epithelial cells. J Immunol 172: 3051–3058.
30. Baird SD, Turcotte M, Korneluk RG, Holcik M (2006) Searching for IRES. RNA 12: 1755–1785.
31. Han B, Dong Z, Zhang JT (2003) Tight control of platelet-derived growth factor B/c-sis expression by interplay between the 5′-untranslated region sequence and the major upstream promoter. J Biol Chem 278: 46983–46993.
32. Prats AC, Prats H (2002) Translational control of gene expression: role of IRESs and consequences for cell transformation and angiogenesis. Prog Nucleic Acid Res Mol Biol 72: 367–413.
33. Battle TE, Frank DA (2002) The role of STATs in apoptosis. Curr Mol Med 2: 381–392.
34. Stark GR, Kerr IM, Williams BR, Silverman RH, Schreiber RD (1998) How cells respond to interferons. Annu Rev Biochem 67: 227–264.
35. Wadler S, Schwartz EL (1990) Antineoplastic activity of the combination of interferon and cytotoxic agents against experimental and human malignancies: a review. Cancer Res 50: 3473–3486.
36. Evan GI, Vousden KH (2001) Proliferation, cell cycle and apoptosis in cancer. Nature 411: 342–348.
37. Wang LH (2004) Molecular signaling regulating anchorage-independent growth of cancer cells. Mt Sinai J Med 71: 361–367.

38. Dhar D, Roy S, Das S (2007) Translational control of the interferon regulatory factor 2 mRNA by IRES element. Nucleic Acids Res 35: 5409–5421.
39. Kaplan DH, Shankaran V, Dighe AS, Stockert E, Aguet M, et al. (1998) Demonstration of an interferon gamma -dependent tumor surveillance system in immunocompetent mice. Proc Natl Acad Sci U S A 95: 7556–7561.
40. Takaoka A, Hayakawa S, Yanai H, Stoiber D, Negishi H, et al. (2003) Integration of interferon-alpha/beta signalling to p53 responses in tumour suppression and antiviral defence. Nature 424: 516–523.
41. Huang S, Bucana CD, Van Arsdall M, Fidler IJ (2002) Stat1 negatively regulates angiogenesis, tumorigenicity and metastasis of tumor cells. Oncogene 21: 2504–2512.
42. Wong LH, Krauer KG, Hatzinisiriou I, Estcourt MJ, Hersey P, et al. (1997) Interferon-resistant human melanoma cells are deficient in ISGF3 components, STAT1, STAT2, and p48-ISGF3gamma. J Biol Chem 272: 28779–28785.
43. Abril E, Real LM, Serrano A, Jimenez P, Garcia A, et al. (1998) Unresponsiveness to interferon associated with STAT1 protein deficiency in a gastric adenocarcinoma cell line. Cancer Immunol Immunother 47: 113–120.
44. von Marschall Z, Scholz A, Cramer T, Schafer G, Schirner M, et al. (2003) Effects of interferon alpha on vascular endothelial growth factor gene transcription and tumor angiogenesis. J Natl Cancer Inst 95: 437–448.
45. Rosewicz S, Detjen K, Scholz A, von Marschall Z (2004) Interferon-alpha: regulatory effects on cell cycle and angiogenesis. Neuroendocrinology 80 Suppl 1: 85–93.
46. Battle TE, Lynch RA, Frank DA (2006) Signal transducer and activator of transcription 1 activation in endothelial cells is a negative regulator of angiogenesis. Cancer Res 66: 3649–3657.
47. Sironi JJ, Ouchi T (2004) STAT1-induced apoptosis is mediated by Caspases 2, 3, and 7. J Biol Chem 279: 4066–4074.
48. Chan AS, Leung SY, Wong MP, Yuen ST, Cheung N, et al. (1998) Expression of vascular endothelial growth factor and its receptors in the anaplastic progression of astrocytoma, oligodendroglioma, and ependymoma. Am J Surg Pathol 22: 816–826.
49. Brown LF, Berse B, Jackman RW, Tognazzi K, Manseau EJ, et al. (1993) Expression of vascular permeability factor (vascular endothelial growth factor) and its receptors in adenocarcinomas of the gastrointestinal tract. Cancer Res 53: 4727–4735.
50. Ben-Asouli Y, Banai Y, Pel-Or Y, Shir A, Kaempfer R (2002) Human interferon-gamma mRNA autoregulates its translation through a pseudoknot that activates the interferon-inducible protein kinase PKR. Cell 108: 221–232.
51. Davis S, Watson JC (1996) In vitro activation of the interferon-induced, double-stranded RNA-dependent protein kinase PKR by RNA from the 3′ untranslated regions of human alpha -tropomyosin. Proc Natl Acad Sci U S A 93: 508–513.
52. Osman F, Jarrous N, Ben-Asouli Y, Kaempfer R (1999) A cis-acting element in the 3′-untranslated region of human TNF-alpha mRNA renders splicing dependent on the activation of protein kinase PKR. Genes Dev 13: 3280–3293.
53. Garcia MA, Gil J, Ventoso I, Guerra S, Domingo E, et al. (2006) Impact of protein kinase PKR in cell biology: from antiviral to antiproliferative action. Microbiol Mol Biol Rev 70: 1032–1060.
54. Rastinejad F, Blau HM (1993) Genetic complementation reveals a novel regulatory role for 3′ untranslated regions in growth and differentiation. Cell 72: 903–917.
55. Gerber HP, Ferrara N (2005) Pharmacology and pharmacodynamics of bevacizumab as monotherapy or in combination with cytotoxic therapy in preclinical studies. Cancer Res 65: 671–680.
56. Presta LG, Chen H, O′Connor SJ, Chisholm V, Meng YG, et al. (1997) Humanization of an anti-vascular endothelial growth factor monoclonal antibody for the therapy of solid tumors and other disorders. Cancer Res 57: 4593–4599.
57. Hurwitz H, Fehrenbacher L, Novotny W, Cartwright T, Hainsworth J, et al. (2004) Bevacizumab plus irinotecan, fluorouracil, and leucovorin for metastatic colorectal cancer. N Engl J Med 350: 2335–2342.
58. Miller KD, Chap LI, Holmes FA, Cobleigh MA, Marcom PK, et al. (2005) Randomized phase III trial of capecitabine compared with bevacizumab plus capecitabine in patients with previously treated metastatic breast cancer. J Clin Oncol 23: 792–799.
59. Los M, Roodhart JML, Voest EE (2007) Target practice: lessons from phase III trials with bevacizumab and vatalanib in the treatment of advanced colorectal cancer. Oncologist 12: 443–450.

Editors' Summary

Background Normally, throughout life, cell division (which produces new cells) and cell death are carefully balanced to keep the body in good working order. But sometimes cells acquire changes (mutations) in their genetic material that allow them to divide uncontrollably to form cancers—disorganized masses of cells. When a cancer is small, it uses the body's existing blood supply to get the oxygen and nutrients it needs for its growth and survival. But, when it gets bigger, it has to develop its own blood supply. This process is called angiogenesis. It involves the release by the cancer cells of proteins called growth factors that bind to other proteins (receptors) on the surface of endothelial cells (the cells lining blood vessels). The receptors then send signals into the endothelial cells that tell them to make new blood vessels. One important angiogenic growth factor is "vascular endothelial growth factor" (VEGF). Tumors that make large amounts of VEGF tend to be more abnormal and more aggressive than those that make less VEGF. In addition, high levels of VEGF in the blood are often associated with poor responses to chemotherapy, drug regimens designed to kill cancer cells.

Why Was This Study Done? Because VEGF is a key regulator of tumor development, several anti-VEGF therapies—drugs that target VEGF and its receptors—have been developed. These therapies strongly suppress the growth of tumor cells in the laboratory and in animals but, when used alone, are no better at increasing the survival times of patients with cancer than standard chemotherapy. Scientists are now looking for an explanation for this disappointing result. Like all proteins, cells make VEGF by "transcribing" its DNA blueprint into an mRNA copy (*vegf* mRNA), the coding region of which is "translated" into the VEGF protein. Other, "noncoding" regions of *vegf* mRNA control when and where VEGF is made. Scientists have recently discovered that the noncoding regions of some mRNAs suppress tumor development. In this study, therefore, the researchers investigate whether *vegf* mRNA has an unrecognized function in tumor cells that could explain the disappointing clinical results of anti-VEGF therapeutics.

What Did the Researchers Do and Find? The researchers first used a technique called small interfering (si) RNA knockdown to stop VEGF expression in human colon cancer cells growing in dishes. siRNAs are short RNAs that bind to and destroy specific mRNAs in cells, thereby preventing the translation of those mRNAs into proteins. The treatment of human colon cancer cells with *vegf*-targeting siRNAs made the cells more sensitive to chemotherapy-induced apoptosis (a type of cell death). This sensitivity was only partly reversed by adding VEGF to the cells. By contrast, cancer cells engineered to make more *vegf* mRNA had increased resistance to chemotherapy-induced apoptosis. Treatment of these cells with an antibody that inhibited VEGF function did not completely block this resistance. Together, these results suggest that both *vegf* mRNA and VEGF protein have anti-apoptotic effects. The researchers show that the anti-apoptotic activity of *vegf* mRNA requires a noncoding part of the mRNA called the 5′ UTR, and that whereas human colon cancer cells expressing this 5′ UTR form tumors in mice, cells expressing a mutated 5′ UTR do not. Finally, they report that the expression of several pro-apoptotic genes and of an anti-tumor pathway known as the interferon/STAT1 tumor suppression pathway is down-regulated in tumors that express the *vegf* 5′ UTR.

What Do These Findings Mean? These findings suggest that some cancer cells have a survival system that is regulated by *vegf* mRNA and are the first to show that a 5′UTR of mRNA can promote tumor growth. They indicate that VEGF and its mRNA work together to promote their development and to increase their resistance to chemotherapy drugs. They suggest that combining therapies that prevent the production of *vegf* mRNA (for example, siRNA-based gene silencing) with therapies that block the function of VEGF might improve survival times for patients whose tumors overexpress VEGF.

Additional Information. Please access these Web sites via the online version of this summary at http://dx.doi.org/10.1371/journal.pmed.0050094.

- This study is discussed further in a *PLoS Medicine* Perspective by Hughes and Jones
- The US National Cancer Institute provides information about all aspects of cancer, including information on angiogenesis, and on bevacizumab, an anti-VEGF therapeutic (in English and Spanish)
- CancerQuest, from Emory University, provides information on all aspects of cancer, including angiogenesis (in several languages)
- Cancer Research UK also provides basic information about what causes cancers and how they develop, grow, and spread, including information about angiogenesis
- Wikipedia has pages on VEGF and on siRNA (note that Wikipedia is a free online encyclopedia that anyone can edit; available in several languages)